Contrib Mineral Petrol (2012) 163:109–131
DOI 10.1007/s00410-011-0661-0

ORIGINAL PAPER

Crystal recycling in the steady-state system of the active Stromboli volcano: a 2.5-ka story inferred from in situ Sr-isotope and trace element data

Lorella Francalanci · Riccardo Avanzinelli · Isabella Nardini · Massimo Tiepolo · Jon P. Davidson · Riccardo Vannucci

Received: 15 January 2011 / Accepted: 26 May 2011 / Published online: 17 June 2011

Abstract In situ Sr-isotope data by microdrilling, coupled with major and trace element analyses, have been performed on plagioclase and clinopyroxene from seven samples collected during the 2002–2003 eruptive crisis at Stromboli volcano (Aeolian Islands, Italy). On 28 December 2002, the persistent moderate explosive activity was broken by an effusive event lasting about 7 months. A more violent explosion (paroxysm) occurred on 5 April 2003. Two magma types were erupted, namely a volatile-poor and highly porphyritic magma (HP-magma) poured out as scoria or lava and a volatile-rich, phenocryst-poor magma (LP-magma) found as pumice. LP-magma differs from the HP-magma also for its slightly less-evolved chemistry, the groundmass composition and the lower Sr-isotope ratios. Micro-Sr-isotope data show the presence of zoned minerals in strong isotope disequilibrium, as previously found in products erupted in 1984, 1985 and 1996 AD, with $^{87}Sr/^{86}Sr$ values generally decreasing from cores to rims of minerals. Only some outer rims testify for equilibrium with the host groundmass. The internal mineral zones with high Sr-isotope ratios (0.70665–0.70618) are interpreted as 'antecrysts', crystallised during the previous activity and recycled in the present-day system since the opening shoshonitic activity of the Recent Period, which occurred at about 2.5 ka ago. This result has implications for the dynamics of the present-day plumbing system of Stromboli at intermediate pressure (about 2–3 km depth) and allows us to propose a model whereby an HP-magma reservoir is directly interconnected at the bottom with a cumulate crystal much reservoir. Efficient mixing between residing HP- and input LP-magmas can occur in this reservoir, due to more similar rheological characteristics of the two magmas than in the conduit, where crystallisation is enhanced by degassing. Antecrysts (and possibly melts) re-enter in the HP-magma reservoir both from the bottom, recycled by ascending LP-magmas crossing the crystal mush, and from the top, recycled by descending degassed and dense HP-magma, residual of the periodic Strombolian explosions at the surface. The isotope variation measured in the groundmasses allows calculating the proportion of the LP-magma entering the shallow HP-magma reservoir at ~20%. From this proportion, we estimate that the total volume of LP-magma input during 2002–2003 closely matches the magma volume erupted in the effusive event, suggesting a steady-state system at broadly constant volume. The comparison with estimates of the LP-magma volume ejected by the paroxysm indicates that the

Communicated by T. L. Grove.

Electronic supplementary material The online version of this article (doi:10.1007/s00410-011-0661-0) contains supplementary material, which is available to authorized users.

L. Francalanci (✉) · R. Avanzinelli · I. Nardini
Dipartimento di Scienze della Terra, Università degli Studi di Firenze, via La Pira, 4, 50121 Florence, Italy
e-mail: lorella.francalanci@unifi.it

L. Francalanci
C.N.R.-I.G.G., Sezione di Firenze, via La Pira, 4, 50121 Florence, Italy

J. P. Davidson
Department of Earth Sciences, University of Durham Science laboratories, South Road, Durham DH1 3LE, UK

M. Tiepolo · R. Vannucci
C.N.R.-I.G.G., Sezione di Pavia, via Ferrata, 1, 27100 Pavia, Italy

R. Vannucci
Dipartimento d Scienze della Terra, Università degli Studi di Pavia, via Ferrata, 1, 27100 Pavia, Italy

LP-magma amount directly reaching the surface during the 5 April paroxysm is minimal with respect to that entering the system.

Keywords Microanalyses · Isotopic microdrilling · Sr-isotope disequilibria · Mineral recycling · Stromboli

Introduction

Mineral/liquid elemental and isotopic disequilibria are often found in volcanic rocks and are useful for revealing pre-eruptive magmatic processes. Bulk rocks frequently represent a mechanical mixture of various phases with possible different origin (e.g., Tepley and Davidson 2003; Davidson et al. 2007 and reference therein; Burgisser and Bergantz 2011). Mineral phases preserve the history of changing physical and chemical conditions during their growth, thus recording more information on processes occurring during the magma ascent to the surface than the whole rocks. Accordingly, in situ mineral determinations of $^{87}Sr/^{86}Sr$ values, associated with major and trace element analyses on core-rim traverses, provide constraints on the timescale of magma uprise and storage, and on the configurations of the volcanic plumbing systems. Both laser ablation (e.g., Davidson et al. 2001; Ramos et al. 2004) and microdrilling techniques (e.g., Tepley III et al. 2000; Perini et al. 2003) have been used for in situ analyses on phenocrysts and associated glasses.

In this study, we present in situ Sr-isotope analyses performed by microdrilling on the products (lavas, scoria and pumices) erupted during the 2002–2003 period at Stromboli Volcano (Aeolian Islands, Italy).

The present-day volcanic activity of Stromboli generally consists of mild explosions, at a rate of 3–5 per hour, ejecting black scoria bombs, lapilli and ash around the craters. This normal 'Strombolian' activity is sometimes interrupted by lava flows and more violent explosions (paroxysms of different scale). The products erupted by these paroxysms interest a larger area than typical Strombolian activity and include small volumes of light coloured pumices, together with scoria and blocks (Rosi et al. 2000; Bertagnini et al. 2008). The 2002–2003 eruptive crisis, characterised by one of the most voluminous lava flow of Stromboli in the past two centuries, represented the most dangerous volcanic crisis occurring in Italy since the 1944 eruption of Vesuvius. The crisis had its peak on 30 December, 2 days after the onset of the lava flow, when the eastern part of the Sciara del Fuoco collapsed, producing a tsunami that devastated the NE coast of the island. Furthermore, about 3 months after the beginning of the lava effusion, on 5 April 2003, a paroxysmal eruption occurred at the summit craters. The lava flow continued for about 7 months, and it was periodically sampled mainly from the active channels (Landi et al. 2006, 2008).

Several recent papers have improved our knowledge of the behaviour of the present-day magmatic system of Stromboli (e.g., Allard et al. 1994, 2010; Francalanci et al. 1999, 2004, 2005; Métrich et al. 2001, 2005, 2010; Landi et al. 2004; Bertagnini et al. 2003, 2008 and references therein), but little is still known on the detailed processes controlling the change from the typical mild explosive activity to the more vigorous paroxysms and lava flow eruptions. In particular, the presence of complex mineral/liquid Sr-isotope disequilibria in products erupted between 1984 and 1996 AD (Francalanci et al. 1999, 2005, 2008) have pointed out the importance of Sr-isotope ratios and in situ micro-Sr-isotope analyses for understanding the dynamics of the present-day volcanic system of Stromboli, leading to propose the possible existence of a cumulus crystal mush zone sited at intermediate depth.

The present paper combines in situ Sr-isotope and major and trace element data of minerals and glassy groundmasses for several samples erupted during the 7 months of 2002–2003 crisis, in order to better understand the isotope disequilibrium processes and to shed lights on the crystal recycling mechanisms and the characteristics of the crystal mush. These results are also useful in improving our understanding of the timescales of pre-eruptive magmatic processes controlling the style of the present-day Strombolian activity.

General background

Stromboli stratovolcano (Fig. 1) is the northernmost island of the Aeolian arc, Southern Tyrrhenian Sea, which is located on 20-km-thick continental crust (Morelli et al. 1975). The volcano has an elevation of 924 m above sea level (m. a.s.l.) and continues for 2,000 m b.s.l. The oldest subaerial rocks (204 ± 25 ka) form the Strombolicchio neck, located NE of Stromboli Island and belonging to the same submarine edifice. Stromboli Island itself rose from the sea about 100 ka ago (Gillot and Keller 1993). The volcanic history of Stromboli was characterised by six main volcano-building periods (from the oldest to the youngest: Paleostromboli I, II, III, Vancori, Neostromboli and Recent; Fig. 1) alternating with volcano-collapsed periods (Francalanci et al. 1993; Hornig-Kjarsgaard et al. 1993). Amongst the eight edifice collapses, the youngest ones led to the formation of the Sciara del Fuoco depression in its present form, on the NW flank of the volcano (Pasquarè et al. 1993; Kokelaar and Romagnoli 1995; Tibaldi 2001).

During the last 200 ka, Stromboli outpoured magmas ranging from calc-alkaline (mainly basaltic-andesites) to

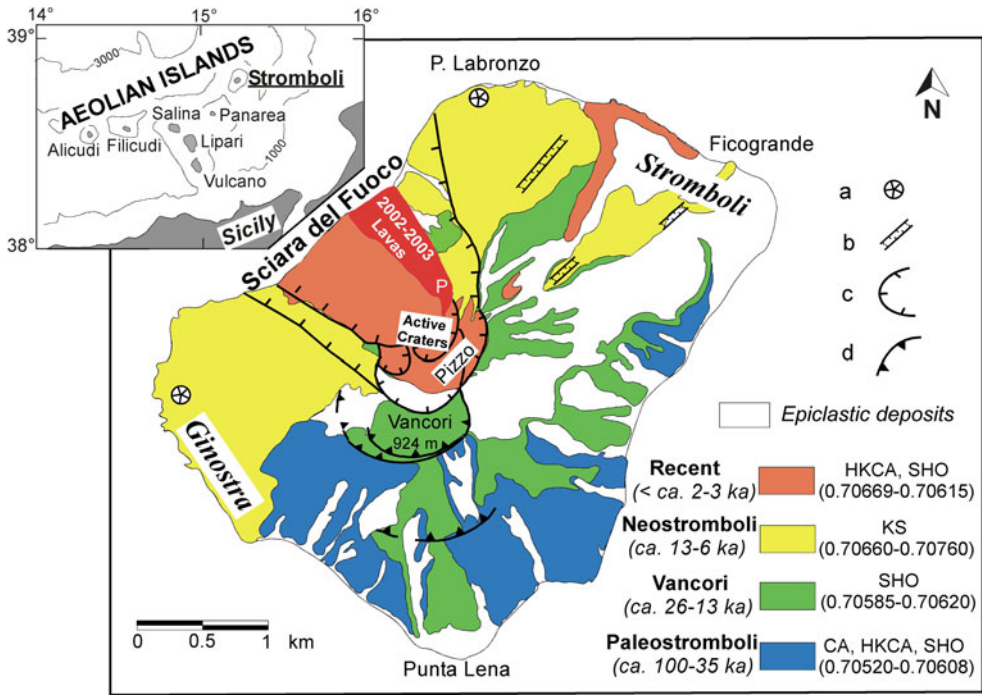

Fig. 1 Simplified geological map of the emerged Stromboli volcano with the reported 2002–2003 lava setting along the Sciara del Fuoco scar. *P* Pianoro; Pizzo: Pizzo-Sopra-la-Fossa. For each *legend-box*, the referred eruptive period (Paleostromboli, Vancori, Neostromboli, Recent), the age in ka, the magmatic series (*CA* calc-alkaline, *HKCA* high-K calc-alkaline, *SHO* shoshonitic, *KS* potassic) and the range of Sr-isotope ratios of the erupted magmas for each period are reported (data from Francalanci et al. 1993, 1999, 2004, 2005; Hornig-Kjarsgaard et al. 1993; Gillot and Keller 1993; Rosi et al. 2000; Speranza et al. 2008; Di Salvo 2010); **a** craters, **b** eruptive fissure, **c** sector collapse, **d** caldera collapse. Map modified after Keller et al. (1993) and Tibaldi (2001). *Inset* on the *left top*: bathymetric map of the Aeolian volcanic arc (Southern Tyrrhenian Sea, Italy) showing the Stromboli location relative to other main islands (in *grey colour*)

potassic-alkaline (potassic leucite-bearing trachybasalts and shoshonites), through high-K calc-alkaline (high-K basalts and andesites) and shoshonitic (shoshonitic basalts to trachytes) (Francalanci et al. 1989, 1993; Hornig-Kjarsgaard et al. 1993). Each period of activity is characterised by a certain chemical affinity. Strombolicchio neck and the products of the Paleostromboli II period (~60 ka) are calc-alkaline. Pyroclastic deposits and lavas erupted during the Paleostromboli I (~85 ka) and III (~35 ka) periods have mainly high-K calc-alkaline compositions, whereas the activity of the Vancori period (~26–13 ka) was mostly characterised by shoshonitic lava flows. Potassic-alkaline lava flows were erupted during the Neostromboli period (~13–6 ka) from central and eccentric vents, which were mainly located in the north-western part of the volcano. Effusive and Strombolian activity, erupting shoshonitic and high-K basalts (e.g. 'Pizzo-Sopra-la-Fossa tuff', 'Post-Pizzo series', 'San-Bartolo lavas' and present-day products), mainly characterise the Recent Period of activity (younger than ~2.5 ka) (Fig. 1) (Hornig-Kjarsgaard et al. 1993; Gillot and Keller 1993; Petrone et al. 2004, 2006; Speranza et al. 2008; Di Salvo 2010).

The variation of magma composition from calc-alkaline to potassic is associated with a general increase in incompatible trace element contents and Sr-isotope ratios, whereas Nd isotope ratios generally decrease. Therefore, the products from each period are well defined by characteristic Sr–Nd isotope signature. Specifically, Sr-isotope ratios are lowest in the calc-alkaline rocks (Strombolicchio: 0.70519–0.70537, and Paleostromboli II periods: 0.70509–0.70537) and highest in the potassic rocks (Neostromboli period), whereas they decrease with time during the Recent Period (Fig. 1) (Francalanci et al. 1989, 1993, 1999, 2004).

Present-day Strombolian activity

The present-day Strombolian activity, which begun between the third and seventh century (Rosi et al. 2000), takes place from several vents in a crater terrace, situated at 750 m a.s.l. on top of the Sciara del Fuoco depression (Fig. 1). The 'normal' mildly explosive activity ejects fountains of blocks, black scoria bombs, lapilli and ash at variable rate of about 3–5 events per hour. Although each crater is characterised by different explosive dynamics, infrasonic, thermal and seismic data indicate that the feeding system is shallow (about 500 m. a.s.l.) and

common to all the vents (Ripepe et al. 2008). Another type of activity consists of a persistent bursting of small gas bubbles (one burst every 1–2 s), which occur at only one vent at once (puffing) (Ripepe et al. 2002, 2008 and references therein).

The normal explosive activity is occasionally interrupted by episodes of lavas flowing into the Sciara del Fuoco lasting from <3 days to 11 months (Barberi et al. 1993). Recent notable effusive events occurred from December 1985 to April 1986 (De Fino et al. 1988), in the 2002–2003 period (Landi et al. 2006, 2008; Spampinato et al. 2008) and from 27 February to 2 April 2007 (Landi et al. 2009).

The present-day activity is also characterised by more violent explosions than the usual ones, generally called paroxysms consisting of impulsive, short-lived blasts from different craters. These are recently classified of small-, intermediate- and large-scale according to their explosion energy (Barberi et al. 1993; Bertagnini et al. 2008; Metrich et al. 2010). Meter-sized scoriaceous bombs and blocks are ejected up to the Pizzo-Sopra-la-Fossa peak by the small-scale paroxysms and up to the coasts by the more energetic paroxysms. The last paroxysms, of intermediate-scale, occurred on 5 April 2003 and 15 March 2007, during the effusive activities. Tsunamis are also generally associated with paroxysmal eruptions and landslides. The last tsunami occurred on 30 December 2002, triggered by landslides related to the lava effusion (Bonaccorso et al. 2003).

A volatile-poor highly porphyritic magma (hereafter the 'HP-magma') is erupted both as black scoria bombs and lapilli by the normal explosive activity and as lava flows. Scoria similar to those of the normal activity (HP-magma) constitute the most voluminous juvenile component erupted by major explosions and paroxysms, whereas the other component is represented by a highly vesiculate light pumice, formed by a volatile-rich magma with low phenocryst content (hereafter the 'LP-magma') (Bonaccorso et al. 1996; Francalanci et al. 1999, 2004; Bertagnini et al. 2003; Métrich et al. 2001). Black scoria and light pumices are usually mingled at various scales.

The 2002–2003 eruptive crisis

The 2002–2003 eruptive crisis consisted of several phenomena such as contemporaneous lava outpouring from multiple vents (28 December 2002–22 July 2003), the paroxysm of 5 April 2003 whilst lava emission was still in progress and the tsunami generated by the collapse of the Sciara del Fuoco flank into the sea.

The effusion started with a short-lived mild explosive episode from a lateral vent, generating a hot avalanche deposit at the base of the Sciara del Fuoco, which was soon followed by the overflow of a transitory exceptionally fluid lava flow from the NE summit crater rim, descending the north-east slope of the Sciara del Fuoco down to the sea. Soon after, less fluid lava was erupted from a vent opened at 600 m a.s.l. in the NE portion of the Sciara del Fuoco (Fig. 1). After the onset of the effusive activity, the draining of lava from lateral vents led to a drop of magma level in the central conduit, to the collapse of the craters and to the cessation of the mild explosive activity (Landi et al. 2006, 2008; Spampinato et al. 2008).

During the first 2 days, the effusion was characterised by relatively high lava discharge rate (Marsella et al. 2008) and by contemporaneous gravity movements in the Sciara del Fuoco. These culminated on 30 December with two tsunamigenic collapses occurring 4 min apart and affecting the eastern sector of the Sciara del Fuoco both above and below sea level (Bonaccorso et al. 2003; Tommasi et al. 2005). Soon after, the effusive activity concentrated in vents located at 550 m elevation within the scar left by the landslide. During January, momentary interruption of the lava flow was soon followed by new lava outpouring from the vents at 600 m. a.s.l. at the foot of the NE cone ('Pianoro'; Fig. 1). On 5 April 2003, a paroxysmal eruption occurred in the summit craters and in the lava field. It was the most violent event of the last 50 years leading to: (a) a fallout deposit of bombs, lithic blocks and ash all over the upper part of the volcano, (b) a fallout deposit of light pumice in the southern flanks of the cone down to the sea, (c) the ejection of meter-sized ballistic blocks along the volcano flanks and on Ginostra village and (d) the accumulation of a thick pyroclastic flow deposit, rich in mingled scoria-pumice bombs, onto the active lava field in the Pianoro. The effusive activity stopped for a couple of hours and then resumed at the edge of the Pianoro (Rosi et al. 2006; Francalanci et al. 2008; Pistolesi et al. 2008; Harris et al. 2008).

Since mid-April 2003, degassing and spatter activity started from the lava vents on Pianoro, resulting in the rapid growth of two hornitos, rising above the lava field at a maximum height of 25 m in July. During the same period, the explosive activity in the central craters also increased. In July, the lava output rate decreased and ended on 22 July. The waning phase of the lava output was accompanied by a rapid rise of the magma in the central conduit and the full resumption of Strombolian activity in all the craters (Puglisi et al. 2005; Ripepe et al. 2005; Landi et al. 2006, 2008). The total lava volume was estimated at 12.5×10^6 m^3, with an average effusion rate of about 0.7 m^3/s (Marsella et al. 2008).

Petrochemical background

Black scoria and lavas (HP-magma) have seriate textures with high phenocryst content (~45–60vol% of phenocrysts and microphenocrysts) and a glassy to

microcrystalline groundmass. The most abundant mineral phase is plagioclase (on average ≈35vol%), followed by clinopyroxene (on average ≈15vol%) and olivine (on average ≈5vol%). Microphenocrysts mostly consist of plagioclase and some olivine (Francalanci et al. 2004, 2005; Landi et al. 2004; Bertagnini et al. 2008).

Clinopyroxene is the largest phase (0.5–5 mm) and ranges from augite to diopside, with Mg# [molar $Mg^{2+}/(Mg^{2+}+Fe^{2+})$] mainly between 0.70 and 0.91. Zoning can be normal or oscillatory, the whole range of compositions being often found within the same crystal. Outer rims are always augitic (Mg# 0.74–0.77), in equilibrium with the groundmass compositions; cores have augitic to diopsidic compositions and are often partially resorbed.

Olivine from HP-magmas commonly ranges between 0.2 and 3 mm in size. It has compositions $Fo_{70–73}$, usually in equilibrium with the groundmasses. Zoning, when present, is weak, normal or reverse.

Plagioclase phenocrysts are between 0.1 and 2.5 mm and show a large compositional range ($An_{60–87}$). The largest plagioclase crystals usually have resorbed cores and complex zoning in the rims, with multiple sieved textures repeated along growth zones. The outer rims, however, are usually An_{65}, in equilibrium with the groundmass composition.

The compositional range of olivine, clinopyroxene and plagioclase HP-magmas has remained nearly the same since the beginning of the twentieth century and, probably, since the beginning of the present-day Strombolian activity (Francalanci et al. 2004, 2005; Landi et al. 2004; Bertagnini et al. 2008).

Light pumice (LP-magma) has a weakly porphyritic seriate texture (<10vol% of crystals, usually ≈5vol%) with a glassy groundmass. The mineral assemblage consists of olivine, clinopyroxene and plagioclase, with variable proportions in different samples. Euhedral crystals, in equilibrium with the glassy groundmass, are usually small (<0.5 mm), whereas the largest minerals are xenocrysts (e.g. crystals in equilibrium with more evolved glasses than pumice glass) (Métrich et al. 2001; Francalanci et al. 2004).

Olivine crystals of the pumice generally have a large compositional range ($Fo_{68–86}$) and complex zoning. The largest crystals are sometimes strongly reversely zoned: cores with Fo_{70} and rims with higher Fo (up to Fo_{86}) contents in equilibrium with the groundmass. A more forsteritic ($Fo_{88–91}$) olivine is erupted during the large-scale paroxysm (Bertagnini et al. 2003, 2008). Clinopyroxene of the pumice shows Mg# between 0.69 and 0.91, similarly to that of the HP-products. Phenocrysts are often oscillatory zoned with the outer rims usually having high Mg# values (0.84–0.91) similar to microphenocrysts and generally in equilibrium with the groundmass composition.

Plagioclase shows a large variation in An content ($An_{60–90}$), but microphenocrysts and the rims of phenocrysts usually have An >80%, in equilibrium with the LP groundmass. Single phenocrysts display strong (e.g. $An_{65–85}$) complex reverse or oscillatory zoning. Cores are often partially resorbed and have variable An contents (Métrich et al. 2001; Francalanci et al. 2004).

Scoria, lavas and pumice erupted since the onset of the Strombolian activity are high-K and shoshonitic basalts. LP-magmas are slightly less evolved than the HP-magmas, with slightly lower silica, K_2O (about 1 and 0.5 wt% of difference, respectively) and incompatible trace element contents, and higher MgO, Co, Ni, V and Sc abundances. The matrix glass compositions of LP- and HP-products are quite distinct. Pumice glasses are shoshonitic basalts, whereas scoria and lava glasses have more evolved compositions with SiO_2 and K_2O contents between 51–53 and 3.5–5.2 wt%, respectively (Francalanci et al. 2004, 2005; Bertagnini et al. 2008).

Sr-isotope ratios of HP-magmas remained nearly constant since the beginning of the twentieth century to around 1980 A.D. (0.70626 ± 2, 2σ). After 1980, $^{87}Sr/^{86}Sr$ smoothly decreases to the value of 0.70615 of the present days (Francalanci et al. 1999, 2004, 2005). $^{87}Sr/^{86}Sr$ values of LP-magmas (≈0.70610) are significantly lower than those of HP-magmas. Nd-isotope ratios of scoria, lavas and pumice show a slight inverse correlation with Sr-isotopes, but their variation is very small (0.51256 ± 1; Francalanci et al. 1999, 2004).

An in situ major and trace element and Sr-isotope microanalysis study was previously performed in four samples representing the 1985–1986 lava flows, a scoria of the 1984 'normal' activity, a scoria and a coeval pumice of the 1996 small-scale paroxysm (Francalanci et al. 2005). This study pointed out the presence of a large and comparable Sr-isotope disequilibrium in plagioclase and clinopyroxene, with HP-magma having cores with either high $^{87}Sr/^{86}Sr$ (≈0.70635) or low $^{87}Sr/^{86}Sr$ (≈0.70614–0.70608). In the former case, the cores are usually resorbed. Low $^{87}Sr/^{86}Sr$ values were also found in the outer cores grown around the more Sr radiogenic cores. Mineral rims and groundmasses generally showed similar and intermediate $^{87}Sr/^{86}Sr$ (≈0.70628–0.70613). The LP-magmas presented similar Sr-isotope crystal zones, but their lowest Sr-isotopes were found in the rims and glassy groundmasses.

State of the art on the dynamics and plumbing system of the present-day activity

Since its inception, Strombolian activity has been dominated by the interplay between magmas having contrasting density and viscosity: the shallow, crystal-rich and degassed magma (HP-magma) and the nearly aphyric, volatile-

rich magma of deeper derivation (LP-magma). These magmas reside in a polybaric multi-reservoir plumbing system and interact in different ways (mingling–mixing) (Francalanci et al. 1999, 2004, 2005).

The LP-magmas are sited at a lithostatic pressure of 190–250 MPa, as derived from the H_2O–CO_2 dissolved contents of melt inclusions in equilibrium olivine (Métrich et al. 2001, 2005, 2010; Bertagnini et al. 2003). These calculated pressures give a magma pond zone located at ~7–10 km depth. The LP-magma reservoir is periodically recharged by a mafic Ca-rich magma with relatively low Sr-isotope ratios (~0.70608) and containing CO_2-rich gas phase (Francalanci et al. 2005; Allard 2010; Métrich et al. 2010).

The quite similar bulk composition of the erupted HP/LP-magmas pairs, regardless of their strongly different crystal and volatile contents, has been interpreted as an example of crystallisation from LP- to HP-magma driven by water loss at low pressure (Métrich et al. 2001; Bertagnini et al. 2003). A shallow reservoir at ~2–3 km was firstly hypothesised in order to explain the homogeneous Sr-isotope data of the HP-magmas (Francalanci et al. 1999), consistently with a possible remnant of an old structure at this pressure level (Vaggelli et al. 2003). A magma storage zone at ~1–3 km depth has been later suggested also on the basis of gas plume composition calculations (Aiuppa et al. 2009; Allard 2010) and of melt inclusion data (Métrich et al. 2010). On the contrary, other authors still propose the existence of a continuous conduit from the deep LP-magma reservoir to the surface (Burton et al. 2007; Schiavi et al. 2010).

The dissolved water content of LP-magma is high enough to prevent plagioclase crystallisation, except at the final stages of its transfer to the surface, when the water loss at lower pressure drives the melt composition towards the stability field of plagioclase (e.g., Francalanci et al. 2004; Landi et al. 2004; Di Carlo et al. 2006; Bertagnini et al. 2008).

Minerals in scoria record strong chemical, isotopic and textural heterogeneity, providing evidence of repeated and discrete arrivals of water-rich, less Sr radiogenic LP-magmas in the shallow system. The HP-magmas, therefore, undergo crystallisation of olivine, pyroxene and plagioclase together with periodic mixing with the refreshing volatile-rich LP-magmas which causes crystal dissolution. An efficient mixing is possible because the HP-magmas in the shallow reservoir are not largely degassed and crystallised when they interact with the LP-magmas, allowing the rheological characteristics of the two magmas to be broadly similar. Further degassing and crystallisation occur as the HP-magmas move through the conduits to the surface, thus reaching their high crystal content. During paroxysms, LP-magmas reach the surface without mixing with HP-magmas, leading to the scoria–pumice mingling typical of paroxysm ejecta (Francalanci et al. 1999, 2004, 2005; Armienti et al. 2007; Fornaciai et al. 2009).

The presence of an intermediate cumulate crystal mush body, recording the highly variable and high Sr-isotope signature of the previous magmas, was also proposed for explaining the large Sr-isotope disequilibrium found in plagioclase and clinopyroxene of products erupted in 1984, 1985 and 1996 (Francalanci et al. 2005). During the periodic magma recharge, LP-magma passes through the cumulate reservoir sampling minerals and transporting them into the shallower reservoir. These minerals can be partially resorbed before a crystal zone in equilibrium with LP-magmas forms around them due to degassing at shallow level.

Sampling and analytical methods

Several lava samples were collected during the whole effusive eruption by periodic samplings performed every 10–15 days. A detailed description of the 29 collected samples is reported in Table 1 of Landi et al. (2006). Several samples derive from the active lava channels within the lava field at 600 m a.s.l.; they were quenched in water after collection. Scoria and pumice erupted from the 5 April paroxysm were also collected.

Modal analyses and major element data from whole rocks, matrix glasses and mineral phases from the collected samples of the 2002–2003 eruptive crisis, together with trace element and Sr–Nd isotope analyses of whole rocks, are reported and discussed by Landi et al. (2006, 2008) and Francalanci et al. (2008). For the purposes of the present paper, we performed our studies on a selected number of samples chosen on the basis of time (representativeness of the entire effusive period: about one sample per month) and field (the preferred samples were those quenched at the active lava channels) criteria. Accordingly, the study was particularly focussed on the lavas of 28 December 2002 (onset lava), 6 March 2003, 14 April, 13/17 May, 20 July 2003 (end lava) and on the scoria and pumice of 5 April 2003 paroxysm. On these samples we performed: (1) core-rim micro-Sr-isotope data of selected plagioclase and clinopyroxene by microdrilling, (2) Sr-isotope ratios of glassy groundmasses by microdrilling and handpicking, (3) Sr-isotope ratios of some separated single crystals, (4) major and trace element data of the selected microdrilled minerals by electron microprobe (EMPA) and laser ablation (LAM), respectively. The most zoned plagioclase and clinopyroxene crystals were chosen for microdrilling analyses from each thin section of the selected samples. Groundmasses were also separated by handpicking for $^{86}Sr/^{88}Sr$ analyses on the lavas of 15 January, 17 February,

Table 1 Sr-isotope ratios in whole rocks, groundmasses and minerals (microdrilled and separated) from the 2002–2003 Stromboli products

Date	Product	Sample	Type	Crystal zone and details	L (mm)	Depth	Trace	$^{87}Sr/^{86}Sr$	$2\sigma \times 10^6$
28 Dec. 2002	Lava	STR12/02a	Whole rock	–	–	(μm)	–	*0.706160**	5
28 Dec. 2002	Lava	STR12/02a	Groundmass	Drilled	–	50	–	0.706161	12
28 Dec. 2002	Lava	STR12/02a	Groundmass	Drilled	–	50	–	0.706147	14
28 Dec. 2002	Lava	STR12/02a	Plagioclase-Pl1	C	1.5	50	–	0.706647	11
28 Dec. 2002	Lava	STR12/02a	Plagioclase-Pl1	OC	1.5	50	–	0.706206	9
28 Dec. 2002	Lava	STR12/02a	Plagioclase-Pl1	OR	1.5	50	–	0.706169	11
28 Dec. 2002	Lava	STR12/02a	Plagioclase-Pl2	C(83.4)	1.5	50	–	0.706243	11
28 Dec. 2002	Lava	STR12/02a	Plagioclase-Pl2	IR(71.0) + R(80.0) + OR(68.6)	1.5	50	IR, OR	0.706177	10
28 Dec. 2002	Lava	STR12/02a	Plagioclase-Pl3	C	1.3	50	–	0.706162	10
28 Dec. 2002	Lava	STR12/02a	Plagioclase-Pl3	OC	1.3	50	–	0.706216	12
28 Dec. 2002	Lava	STR12/02a	Plagioclase-Pl3	IR	1.3	50	–	0.706169	11
28 Dec. 2002	Lava	STR12/02a	Plagioclase-Pl3	R	1.3	50	–	0.706176	11
28 Dec. 2002	Lava	STR12/02a	Plagioclase-Pl4	C(80.6)	1.2	50	–	0.706195	16
28 Dec. 2002	Lava	STR12/02a	Plagioclase-Pl4	OC(72.3) + IR(65.8)	1.2	50	IR	0.706196	11
28 Dec. 2002	Lava	STR12/02a	Plagioclase-Pl4	R(81.9) + OR(64.7)	1.2	60	OR	0.706149	11
28 Dec. 2002	Lava	STR12/02a	Clinopyroxene	Separated single crystal	–	–	–	0.706313	7
28 Dec. 2002	Lava	STR12/02a	Clinopyroxene-Cpx13	IR(0.73) + R + OR(0.75)	4.5	50	IR,R,OR	0.706184	10
28 Dec. 2002	Lava	STR12/02b	Whole rock	–	–	–	–	*0.706163**	4
28 Dec. 2002	Lava	STR12/02b	Groundmass	Separated	–	–	–	0.706158	4
15 Jan. 2003	Lava	STR150103	Whole rock	–	–	–	–	*0.706163**	5
15 Jan. 2003	Lava	STR150103	Groundmass	Separated	–	–	–	0.706156	5
1 Feb. 2003	Lava	STR010203	Whole rock	–	–	–	–	*0.706152**	6
17 Feb. 2003	Lava	STR170203	Whole rock	–	–	–	–	*0.706160**	7
17 Feb. 2003	Lava	STR170203	Groundmass	Separated	–	–	–	0.706149	8
4 March 2003	Lava	STR040303	Whole rock	–	–	–	–	*0.706154**	6
6 March 2003	Lava	STR060303	Groundmass	Drilled	–	70	–	0.706150	11
6 March 2003	Lava	STR060303	Plagioclase-Pl2	C	1.6	60	–	0.706283	12
6 March 2003	Lava	STR060303	Plagioclase-Pl2	OR	1.6	60	–	0.706229	16
6 March 2003	Lava	STR060303	Plagioclase-Pl2	IR	1.6	60	–	0.706227	20
6 March 2003	Lava	STR060303	Plagioclase-Pl2	R	1.6	60	–	0.706187	14
6 March 2003	Lava	STR060303	Plagioclase-Pl3	OC	1.2	60	–	0.706207	11
6 March 2003	Lava	STR060303	Plagioclase-Pl3	R	1.2	60	–	0.706171	9
6 March 2003	Lava	STR060303	Plagioclase-Pl4	C	2.5	60	–	0.706143	11
6 March 2003	Lava	STR060303	Plagioclase-Pl4	R	2.5	60	–	0.706189	9
18 March 2003	Lava	STR180303	Groundmass	Separated	–	–	–	0.706151	7
5 April 2003	Scoria	STR050403hi	Groundmass	Separated	–	–	–	0.706150	7
5 April 2003	Scoria	STR050403hS	Plagioclase-Pl1hS	OC(76.9)	1.0	60	OC,R	0.706209	9
5 April 2003	Scoria	STR050403hS	Olivine	Separated single crystal	–	–	–	0.706146	8
5 April 2003	Scoria	STR050403f	Plagioclase-Pl1	C	1.5	60		0.706148	22
5 April 2003	Scoria	STR050403f	Plagioclase-Pl1	OC(67.0)	1.5	60	OC	0.706261	16
5 April 2003	Scoria	STR050403f	Plagioclase-Pl1	IR(81.1) + R	1.5	60	IR	0.706167	14
5 April 2003	Scoria	STR050403f	Plagioclase-Pl3	C(66.0)	0.7	70	C	0.706401	11
5 April 2003	Scoria	STR050403f	Plagioclase-Pl3	R(66.1)	0.7	70	R	0.706183	9
5 April 2003	Scoria	STR050403f	Clinopyroxene-Cpx1	C(0.75) + OC(0.89)	2.5	70	OC	0.705966	12
5 April 2003	Scoria	STR050403f	Clinopyroxene-Cpx1	IR + R(0.76) + OR	2.5	70	IR,R	0.706147	10
5 April 2003	Pumice	STR050403k	Whole rock	–	–	–	–	0.706098	7
5 April 2003	Pumice	STR050403hP	Whole rock	–	–	–	–	0.706111	7
5 April 2003	Pumice	STR050403hP	Groundmass	Separated	–	–	–	0.706116	5
5 April 2003	Pumice	STR050403hP	Plagioclase-Pl2hP	OC(67.5)	1.5	60	C,OC	0.706234	15
5 April 2003	Pumice	STR050403hP	Plagioclase-Pl2hP	R(63.9)	1.5	60	–	0.706290	8

Table 1 continued

Date	Product	Sample	Type	Crystal zone and details	L (mm)	Depth	Trace	$^{87}Sr/^{86}Sr$	$2\sigma \times 10^6$
14 April 2003	Lava	STR140403	Whole rock	–	–	–	–	*0.706156**	8
14 April 2003	Lava	STR140403	Groundmass	–	–	–	–	0.706151	7
14 April 2003	Lava	STR140403	Plagioclase	Separated single crystal	–	–	–	0.706183	6
14 April 2003	Lava	STR140403	Olivine	Separated single crystal	–	–	–	0.706193	8
13 May 2003	Lava	STR130503	Whole rock	–	–	–	–	*0.706156**	6
13 May 2003	Lava	STR130503	Groundmass	Separated	–	–	–	0.706139	6
13 May 2003	Lava	STR130503	Plagioclase-Pl1	OC(65.2)	2.1	60	–	0.706223	11
13 May 2003	Lava	STR130503	Plagioclase-Pl1	IR(67.3)	2.1	60	–	0.706228	11
13 May 2003	Lava	STR130503	Plagioclase-Pl1	R(66.0)–OR(71.6)	2.1	60	–	0.706278	22
13 May 2003	Lava	STR130503	Plagioclase-Pl2	C	1.3	60	–	0.706218	12
13 May 2003	Lava	STR130503	Plagioclase-Pl2	OR	1.3	60	–	0.706218	15
13 May 2003	Lava	STR130503	Clinopyroxene	Separated single crystal	–	–	–	0.706148	8
17 May 2003	Lava	STR170503	Whole rock	–	–	–	–	0.706157	7
17 May 2003	Lava	STR170503	Groundmass	Drilled	–	70	–	0.706142	12
17 May 2003	Lava	STR170503	Plagioclase-Pl1	C(70.5)	1.5	60	C	0.706243	13
17 May 2003	Lava	STR170503	Plagioclase-Pl1	OC(66.7)	1.5	60	OC,R	0.706200	10
17 May 2003	Lava	STR170503	Plagioclase-Pl2	R(68.9) + OR	2.0	60	C,OC,R	0.706200	9
17 May 2003	Lava	STR170503	Plagioclase-Pl3	C(66.6)	1.5	60	OC	0.706202	12
17 May 2003	Lava	STR170503	Plagioclase-Pl3	R(63.6)	1.5	60	R	0.706224	11
17 May 2003	Lava	STR170503	Clinopyroxene	Separated single crystal	1.5	–	–	0.706225	12
17 May 2003	Lava	STR170503	Olivine	Separated single crystal	1.2	–	–	0.706143	12
17 May 2003	Lava	STR170503	Clinopyroxene-Cpx2	C(0.75)	2.0	70	C,OC	0.706210	12
17 May 2003	Lava	STR170503	Clinopyroxene-Cpx2	R + OR(0.75)	2.0	70	R	0.706180	12
6 June 2003	Lava	STR060603	Whole rock	–	–	–	–	*0.706149**	7
3 July 2003	Lava	STR030703	Whole rock	–	–	–	–	*0.706150**	8
3 July 2003	Lava	STR030703	Groundmass	Separated	–	–	–	0.706141	6
20 July 2003	Lava	STR200703	Whole rock	–	–	–	–	*0.706146**	7
20 July 2003	Lava	STR200703	Groundmass	Separated	–	–	–	0.706134	7
20 July 2003	Lava	STR200703	Plagioclase-Pl1	R + OR(58.4)	0.7	50	C,R	0.706150	9
20 July 2003	Lava	STR200703	Plagioclase-Pl2	C(77.5)	0.8	50	–	0.706377	11
20 July 2003	Lava	STR200703	Plagioclase-Pl2	R(66.6) + OR	0.8	50	IR,R	0.706305	12
20 July 2003	Lava	STR200703	Plagioclase-Pl3	C + OC	1.5	60	–	0.706200	8
20 July 2003	Lava	STR200703	Plagioclase-Pl3	IR + R + OR	1.5	50	–	0.706173	11
20 July 2003	Lava	STR200703	Clinopyroxene	Separated single crystal	–	–	–	0.706179	9

L lenght of crystal, *DEPTH* depth of drilling, *TRACE* zones analysed for trace elements. Asterisks and italics: data from Landi et al. (2006)

C core, *OC* outer core, *IR* inner rim, *R* rim, *OR* outer rim; numbers in brackets indicate anorthite content and Mg# [molar $Mg/(Mg + Fe^{2+})$] for plagioclase and clinopyroxene, respectively. "–": no significant or available data. All the data from microdrilling are those with reported DEPTH

18 March and 3 July. Sr-isotope data are reported on Table 1, whereas the other data are published in electronic format (EMPA data on Tables E-1, E-2, LAM data on Tables E-3, E-4a,b).

EMPA–WDS analyses

Major element analyses of plagioclase, clinopyroxene and glassy groundmass were performed by the Jeol JXA 8600 superprobe at the CNR-IGG in Florence. Operating conditions were 15 kV accelerating voltage, 10nA beam current (monitored on a Faraday cup) and variable counting times for major and minor elements. The applied matrix correction method is according to Bence and Albee (1968). In order to avoid or minimise alkali loss, we used a defocused beam (10 μm) and a lower counting time for Na, measuring both Na and K at the beginning of each analyses. Detailed description of analytical procedure with precision and accuracy of measurements are provided by Vaggelli et al. (1999). Natural silicate minerals and glasses were mostly used as primary and secondary standards, whereas a repeatedly analysed polished section (STR09/96e, glass composition reported in Francalanci et al. 2004) from the present-day activity of Stromboli was used for further checking of precision and for allowing more detailed comparisons between different samples.

LAM-ICP MS analyses

The trace element composition of micromilled clinopyroxene and plagioclase crystals was determined by laser ablation ICP-MS at the C.N.R.-I.G.G.-U.O.S. of Pavia. The instrument couples a 266-nm Nd:YAG laser microprobe (Brilliant, Quantel) to a quadrupole ICPMS (DRCe from PerkinElmer). Selected masses were acquired in peak jumping mode, and each analysis consisted in the acquisition of 1 min of background signal and 1 min of ablation signal. NIST-SRM612 was used as external standard, whereas ^{43}Ca was adopted as internal standard. In each analytical run, the USGS reference sample BCR2 was analysed together with unknowns for quality control; precision and accuracy are better than 5 and 10%, respectively. Data reduction was carried out with the software package GLITTER (van Achterbergh et al. 2001).

Micro-Sr-isotope analyses

Olivine and clinopyroxene were separated at the CNR-IGG in Pisa for Sr-isotope analyses. After crushing and sieving, samples were separated into 1000-, 500-, 250- and 160-μm grain sizes. Mineral separates were obtained firstly using a Frantz magnetic separator, purified by handpicking under binocular microscope, then cleaned ultrasonically and dried with pure acetone. Some groundmasses were separated by handpicking from the crushed whole-rock samples.

In situ Sr-isotope microanalyses were performed on glassy groundmasses and on plagioclase and clinopyroxene crystals by microdrilling technique (Fig. 2) using a New Wave™ MicroMill™. Micromilling and extraction of strontium at the nanogram level were carried out following the method proposed by Charlier et al. (2006) at the Department of Earth Sciences, Durham University, UK. Sample loading and mass spectrometry were executed at the Department of Earth Sciences, University of Florence, IT.

We chose 60- to 150-μm polished thick sections for micromilling. Prior to microsampling, optical investigations and in situ analyses of major and trace elements were carried out by electron microprobe and LAM-ICP-MS in order to check the typical and most extreme element zoning. Information on the Sr content at the sample sites allowed us to determine the sample volume needed for each zone to be milled.

Tungsten carbide conical drill bits were used for milling samples from thick sections at depths varying from 50 and 70 μm. The efficiency of the recovery (based on comparing calculated sample mass from the excavation geometry to the actual mass of sample) was in the range of 80–85%.

The purification of strontium was carried out using micro-columns for standard chemical separation technique (SrSpec™ resin). Blank contamination levels were monitored regularly, and the resulting extremely low Sr blank value (~12 pg) did not require any significant correction, considering the amount of Sr processed (3–15 ng).

Sr was loaded on single Re filaments 'sandwiching' 1 μL of sample (taken up in nitric acid) between two small aliquots of TaF5 activator (Charlier et al. 2006). Sr-isotope ratios were measured on the Thermal Ionisation Mass Spectrometer Finnigan Triton TI© (TIMS). ^{87}Sr/^{86}Sr values were measured statically and corrected using an exponential

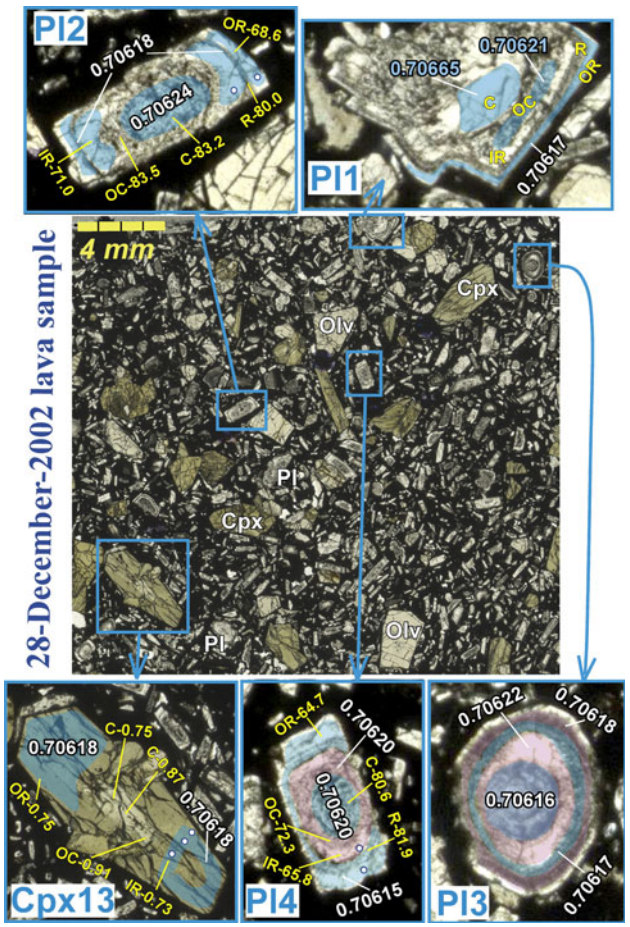

Fig. 2 Scanner image of a polished thin section (60 μm thick) from the 28 December 2002 lava sample (STR1202a) (onset lavas), with enlarged pictures of the minerals microdrilled for Sr-isotope ratios. The name of the minerals is reported on each picture. *Pl* plagioclase, *Cpx* clinopyroxene, *Olv* olivine. The differently coloured areas on the enlarged minerals show the crystal zones micromilled for Sr-isotope analyses on each mineral. The obtained ^{87}Sr/^{86}Sr value for each micromilled zone is also reported in *white colour*. The *two blue* areas of Cpx13 are treated as a single micro-sample; the same is true for the two external *blue areas* of Pl2. *Yellow labels* (*C* core, *OC* outer core, *IR* inner rim, *R* rim, *OR* outer rim) and numbers (An content wt% of plagioclase or Mg# of clinopyroxene) refer to crystal zones recognised by textural and major element data. The *white spots* in Pl2, Cpx13 and Pl4 indicate LAM-ICP-MS analyses

mass fractionation law to $^{86}Sr/^{88}Sr = 0.1194$, respectively, as described by Avanzinelli et al. (2005). Replicate measurements of a low Sr NBS 987 (0.710249, Thirlwall 1991) standard (10 ng of Sr) were performed in order to match the low abundances loaded for Stromboli samples, yielding a mean value of $^{87}Sr/^{86}Sr = 0.710249 \pm 0.000021$ (2σ, $n = 36$). Excluding the first ten measurements used to optimise the loading technique, the remaining data yield a much better reproducibility (i.e. 0.710250 ± 0.000014, 2σ, $n = 26$). Long-term reproducibility on greater-size (150 ng of Sr) NBS 987 standard was $^{87}Sr/^{86}Sr = 0.710250 \pm 0.000012$ (2σ, $n = 147$).

Compositional characteristics of the 2002–2003 products

Lavas and scoria samples collected during the 2002–2003 eruptive crises do not show significant variations with respect to HP-magmas erupted during the previous decades in terms of petrography and composition of whole rocks and groundmasses. They are shoshonitic basalts bearing 45–55vol% of phenocrysts and microphenocrysts of plagioclase (28–36vol%), clinopyroxene (10–16vol%) and olivine (4–7vol%). The same holds true for mineral chemistry data. Plagioclase is $An_{90–60}$, clinopyroxene is diopside–augite in composition (Mg#: 0.72–0.92) and olivine $Fo_{69–74}$. The oscillatory chemical zoning and the solid/liquid equilibrium compositions of each mineral phase (Landi et al. 2006, 2008 and references therein) are similar to those of the previous products (Francalanci et al. 2004; Landi et al. 2004).

Time variations of whole-rock major and trace element contents during the 2002–2003 effusive events are very small. Only a slight decrease in the most incompatible trace element contents is evident after the 5 April paroxysm (Landi et al. 2006, 2008 and references therein).

The pumices (LP-magma) erupted by the 5 April paroxysm have whole-rock, matrix glass and mineral compositions generally similar to those of their analogues from previous paroxysms. The 2003 pumices, however, do not contain stable high-MgO olivine, typical of large-scale paroxysms, and have slightly lower compatible element contents than the previously erupted pumices (Métrich et al. 2005; Francalanci et al. 2008).

Sr-isotope and trace element results

Sr-isotope ratios of whole rocks (Landi et al. 2006) and groundmasses (this study) of lavas slightly decrease with time, passing from 0.706163 ± 5 to 0.706146 ± 7 and from 0.706161 ± 12 to 0.706134 ± 7, respectively (Fig. 3; Table 1). Only the onset lavas (both whole rock and groundmass) have $^{87}Sr/^{86}Sr$ similar to the HP-products erupted during the 1994–2002 period (Fig. 3). The decrease in isotope ratios begins in February 2003 and is more accentuated after the paroxysm, as evident in the groundmasses from May. Groundmasses generally have slightly lower Sr-isotopes than the respective whole rocks.

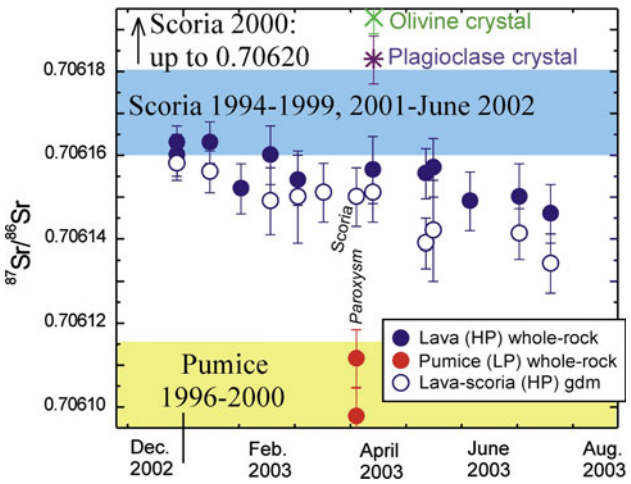

Fig. 3 Sr-isotope ratios of whole-rocks (*blue full symbols*) and groundmasses (gdm; *blue open symbol*) versus time for the products erupted during the effusive event (28 December 2002–22 July 2003) and the paroxysm (5 April 2003). Data for single crystals of olivine and plagioclase are handpicked from the 14 April 2003 lava sample. The coloured fields refer to Sr-isotope range of LP-magmas (*yellow*) and HP-magma (*blue*) from previous activity. The 2000 scoria have a higher $^{87}Sr/^{86}Sr$ than other HP-magmas (up to 0.70620). Before 1994 (not shown) and during the entire twentieth century, scoria and lavas had higher $^{87}Sr/^{86}Sr$ up to 0.70626 (data of fields are from Francalanci et al. 1999, 2004, 2005 and unpublished)

The matrix glass of the scoria (HP-magma) erupted by the 5 April paroxysm has Sr-isotope ratios similar to those of the groundmass of lavas erupted in the time span from 2 months before to 9 days after the paroxysm. The $^{87}Sr/^{86}Sr$ of pumice (LP-magma) is lower than that of the HP-products and similar to that of LP-products erupted by previous paroxysms of the 1996–2000 period (Fig. 3; Table 1).

For the purposes of mineral microanalysis, the analysed crystals have been generally subdivided in hypothetical zones that, from the most internal to the most external part, are called ‘core, outer core, inner rim, rim and outer rim’. These zones are commonly defined by compositional zoning or by variable sieved textures of the crystal analysed. The microdrilled crystal area, however, did not always interest the single zones but, sometimes, included different zones of the crystals. A clear example of this is evident in Pl2 of Fig. 2 for the 28 December 2002 lava sample. The Sr-isotope value for the external zone (blue area at 0.70618) includes three zones recognised on the basis of texture and An content (i.e. an outer rim with

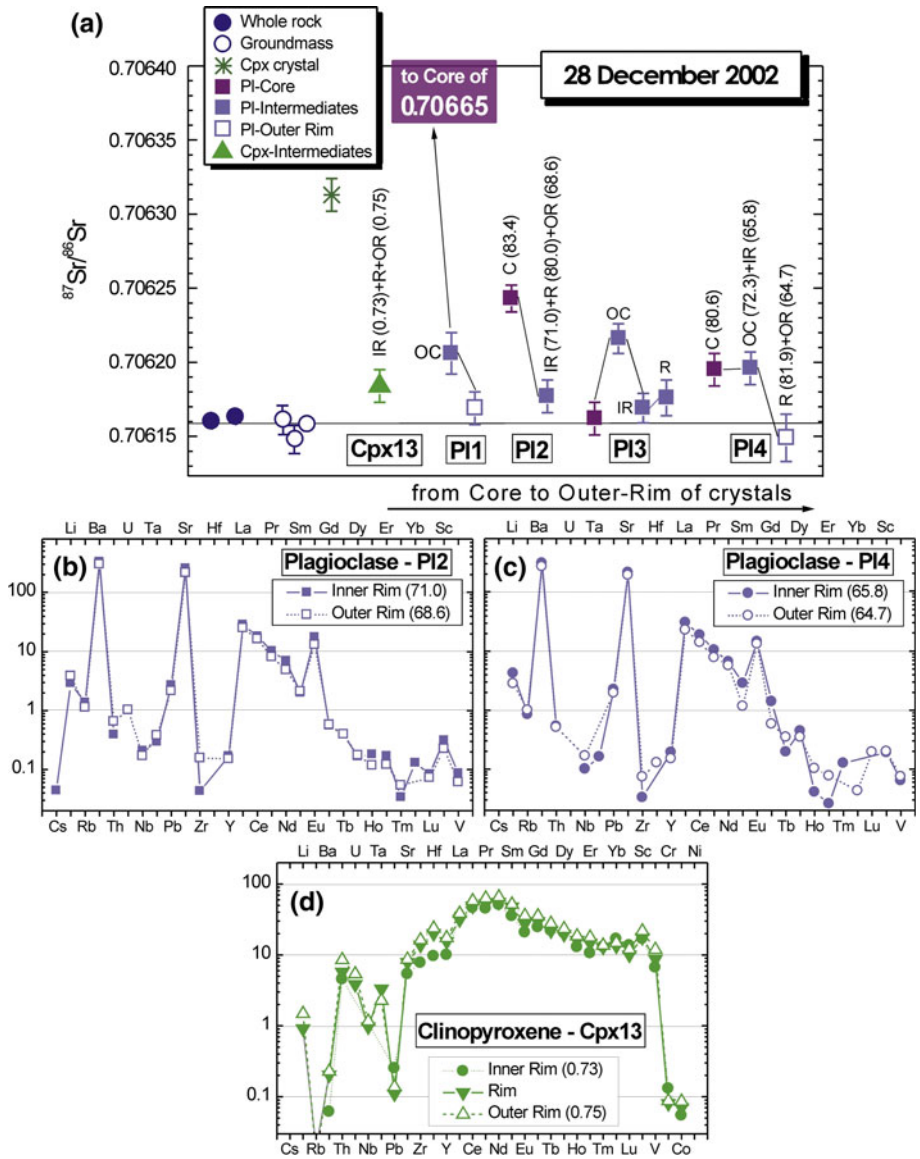

Fig. 4 **a** Micro-Sr-isotope ratios for core-rim traverses in clinopyroxene (Cpx: *triangles*) and plagioclase (Pl: *squares*) of the 28 December 2002 lava sample (STR1202a). Sr-isotope data on a separated clinopyroxene (*asterisk*), whole-rocks (*full circle*) and groundmasses (*open circle*) are also reported (Table 1). *Full violet-squares* = plagioclase cores; *full light-violet-squares* and *green triangle* = intermediate zones; *open light-violet-squares* = prevalent outer rims. *C* core, *OC* outer core, *IR* inner rim, *R* rim, *OR* outer rim. Numbers in *parentheses* indicate the Mg# [mole Mg/(Mg + Fe)] of clinopyroxene and the An% of plagioclase for the referred crystal zone. **b**, **c**, **d** Chondrite-normalised trace element patterns for plagioclase (Pl2, Pl4) and clinopyroxene (Cpx13). Values on the *vertical axes* are rock/chondrite (Anders and Grevesse 1989). An% for plagioclase and Mg# for clinopyroxene of the analysed zones are also given in *parentheses* in the legends. Element ordering: REE have been reported separately from the other elements, which are in order of increasing compatibility into a basaltic mineral assemblage

$An_{68.6}$, a rim with An_{80} and an inner rim with An_{71}), whereas the drilled core (internal blue area at 0.70624) is only represented by a single zone (core with $An_{83.2}$). The area between core and inner rim, called outer core, with the same An content of the core, has not be drilled. In other cases, however, as in the plagioclases Pl3 and Pl1, the milled zones are narrow and well defined (Figs. 2, 4a).

Micro-Sr-isotope analyses show a large isotopic variability (overall between 0.706647 ± 11 and 0.705966 ± 12), even within a single sample, and a persistent isotopic disequilibrium both inside the crystals and between mineral and groundmass. These characteristics are found in all the samples analysed and especially in those from the post-paroxysm lavas. Indeed, in the pre-paroxysm lava samples and syn-paroxysm scoria, the analysed crystal outer rims generally have $^{87}Sr/^{86}Sr$ values similar to those of the groundmass (Figs. 4a, 5a, 6a). On the contrary, in the post-paroxysm lava samples, all the analysed crystal zones usually have $^{87}Sr/^{86}Sr$ values higher than those of both the groundmass and the whole rocks (Figs. 5b, 7a, 8a).

About two-thirds of the microdrilled plagioclase crystals display the same trend of decreasing $^{87}Sr/^{86}Sr$ from core to outer rims, whereas in the other plagioclases, the highest $^{87}Sr/^{86}Sr$ is generally found in the intermediate zones between cores and outer rims (e.g. plagioclase-Pl3 of Fig. 4).

In the 28 December 2002 lava sample (the onset lava), a single core of plagioclase (plagioclase-Pl1 of Fig. 4a) shows a particularly high $^{87}Sr/^{86}Sr$ value of 0.70665. On the other hand, the internal part of the clinopyroxene-Cpx1 of the 5 April 2003 scoria, including a large diopsidic outer core (Mg# = 0.89), has a quite low $^{87}Sr/^{86}Sr$ value

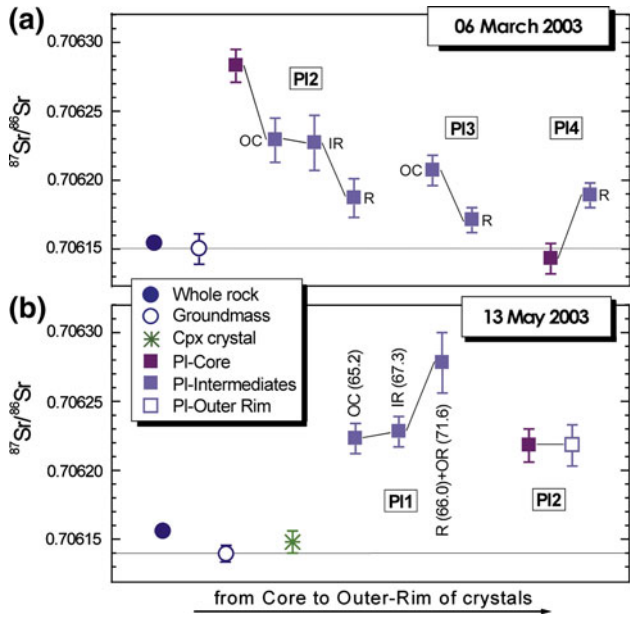

Fig. 5 Micro-Sr-isotope ratios for core-rim traverses in clinopyroxene and plagioclase of **a** the 06 March 2003 lava sample (STR060303 and STR040303) and **b** 13 May 2003 lava sample (STR130503). Sr-isotope data on a separated clinopyroxene (*asterisk*), on whole-rocks (*full circle*) and groundmasses (*open circle*) are also reported. Symbols and labels as in Fig. 4

(0.70597), whereas its outer rim is in equilibrium with the groundmass (Fig. 6a; Table 1). The plagioclase-Pl2hP, found in the pumice, displays isotopic characteristics similar to those of the other microdrilled plagioclase crystals and probably represents a crystal included in the LP-magma during the explosive eruption.

As for the separated single crystals, two of the three analysed olivine crystals are in equilibrium with the groundmass, with the sole exception of crystal from the 14 April 2003 lava sample, whilst three-fourths of the analysed clinopyroxene crystals have more Sr-radiogenic than their groundmasses (Figs. 3, 4, 5, 6, 7, and 8; Table 1).

Trace element analyses were performed on crystal zones without sieved textures or fluid inclusions. Chondrite-normalised (Anders and Grevesse 1989) patterns for these data are plotted in Figs. 4, 6, 7 and 8, together with the respective micro-Sr-isotope data. Plagioclases are mostly enriched in Ba, Sr, Eu and LREE (light rare-earth elements) with respect to chondrite. Clinopyroxene patterns are particularly enriched (>10 times chondrite values) in Hf, Zr, Sc and REE, which show a bell-shaped pattern and negative Eu anomalies (0.7–0.8) (Tables E-3, E-4a,b).

No correlation seems to be present in plagioclases between An contents and trace element characteristics, whereas in the clinopyroxenes, the higher Mg# of outer cores is correlated with the lower trace element contents, the lack of Eu anomaly and the less fractionated LREE (Cpx1 of Fig. 6e and Cpx2 of Fig. 7e).

Discussion

The microanalyses on the products erupted during the 2002–2003 eruptive crisis reported in this study show a more complex system than that previously suggested on the basis of the whole-rock data (e.g., Métrich et al. 2005; Landi et al. 2006, 2008; Francalanci et al. 2008). Indeed, the feeding system of Stromboli volcano results homogeneous at the large scale, but heterogeneous at the small scale, a characteristic that is being increasingly found in many volcanoes (e.g., Davidson et al. 2007; Burgisser and Bergantz 2011).

Comparing the Sr-isotope data of whole-rock/groundmass pairs of the samples analysed, it is evident that in most of the samples, especially starting from May 2003, the groundmass has systematically lower Sr-isotope ratios. On the other hand, all the analysed samples contain phenocrysts in isotopic disequilibrium with the groundmass, having generally higher Sr-isotope values (up to 0.70665; Fig. 4a), but also lower $^{87}Sr/^{86}Sr$ as the case of the Cpx1 core of 5 April 2003 scoria (0. 0.70597; Fig. 6a). Obviously, only the separated minerals and crystal outer rims having $^{87}Sr/^{86}Sr$ value similar to that of the respective groundmass are in equilibrium with the host liquid. In the following sections, these data will be discussed in the light of the previously summarised knowledge on the volcano dynamics and plumbing system configuration at Stromboli ('State of the art on the dynamics and plumbing system of the present-day activity').

Significance and age of the high Sr-isotope crystal zones

Cores of plagioclase and clinopyroxene crystals with higher Sr-isotope ratios than those of the groundmass values (up to 0.70635) were already reported by Francalanci et al. (2005) for samples of 1984, 1985 and 1996 products. These data led to suggest the presence of a cumulate crystal mush reservoir formed during the previous activity (Francalanci et al. 2005). The crystals of this mush can be termed 'antecrysts' (Davidson et al. 2007), having grown in and recycled from closely related progenitor magmas.

The results reported in the present paper indicate the antecrysts, generally found as inner and resorbed parts of the most zoned phenocrysts, are still present on the 2002–2003 Stromboli magmas (Figs. 2, 4, 5, 6, 7 and 8). Furthermore, the measurements, within the 2007 lavas, of bulk minerals with higher $^{87}Sr/^{86}Sr$ than their host groundmass (Landi et al. 2009) indicate the presence of antecrysts also in the most recent products. The occurrence of recycled minerals inherited from the previous activity, therefore, is not a phenomenon of a specific period, but it is

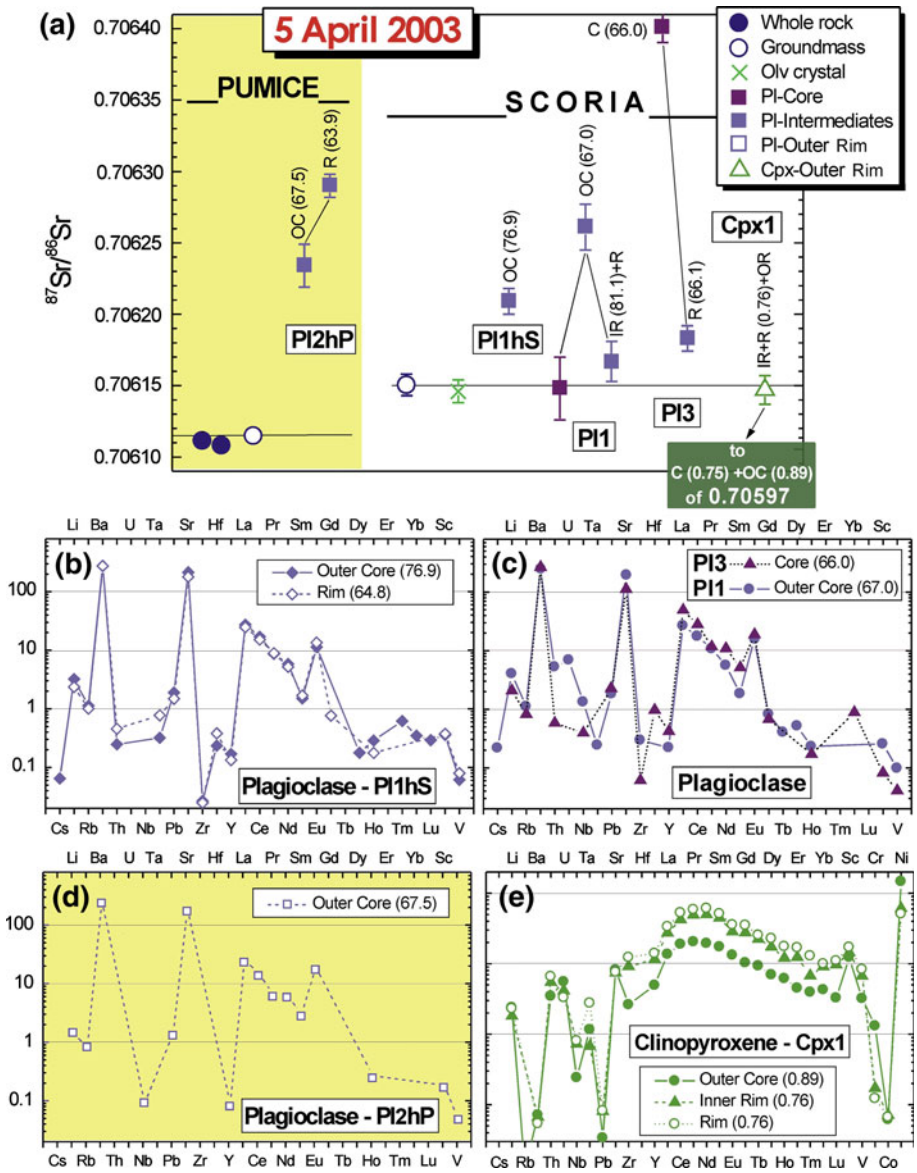

Fig. 6 **a** Micro-Sr-isotope ratios for core-rim traverses in clinopyroxene and plagioclase of the 5 April 2003 pumice (*yellow area*, STR050403hP) and scoria (*white area*, STR050403hS and STR050403f). Sr-isotope data on a separated olivine (Olv) (*cross*), on whole rock (*full circle*) and separated groundmasses (*open circle*) are also reported. Symbols and labels as in Fig. 4. Pl1, Pl3, Pl1hS, Pl2hP and Cpx1 are crystals also analysed for trace elements by LAM-ICP-MS and reported in Fig. 6b, c, d, e. **(b**, **c**, **d**, **e)** Chondrite-normalised trace element patterns for plagioclase crystals (**b**, **c**, **d**) and clinopyroxene (**e**). See caption of Fig. 4 for details

an ubiquitous characteristic of the present-day plumbing system of Stromboli.

The high $^{87}Sr/^{86}Sr$ of the antecrysts provides constraints on the period of activity during which they crystallised. The subaerial rocks of Stromboli have variable Sr-isotope ratios (Fig. 1) with the highest values, ranging between 0.70660 and 0.70760, found in the potassic rocks of the Neostromboli Period (13–6 ka). Starting from the end of this period and throughout the following Recent Period, the $^{87}Sr/^{86}Sr$ values of the erupted products generally decreased with time until the present days, starting from 0.70669 ('Pizzo-Sopra-la-Fossa tuff') to 0.70615 (current volcanic activity). The antecrysts of the 2002–2003 rocks have an Sr-isotope range between 0.70665 and 0.70617, which perfectly encompasses all the values of the Recent Period products. The highest antecryst value of 0.70665, however, could also record the Neostromboli activity (13–6 ka), hence indicating possible recycling of older crystals. Nevertheless, Neostromboli rocks are potassic trachybasalts with higher trace element and potassium contents than the shoshonitic basalts of the Recent Period. Accordingly, comparing the trace element composition of minerals, it is possible to exclude the Neostromboli period for the provenance of these antecrysts (Fig. 9). Indeed, K_2O of plagioclase and trace element contents of clinopyroxene of the 2002–2003 products do not overlap the compositional field of the potassic rock minerals (i.e. KS series of Neostromboli Period), but they show the typical

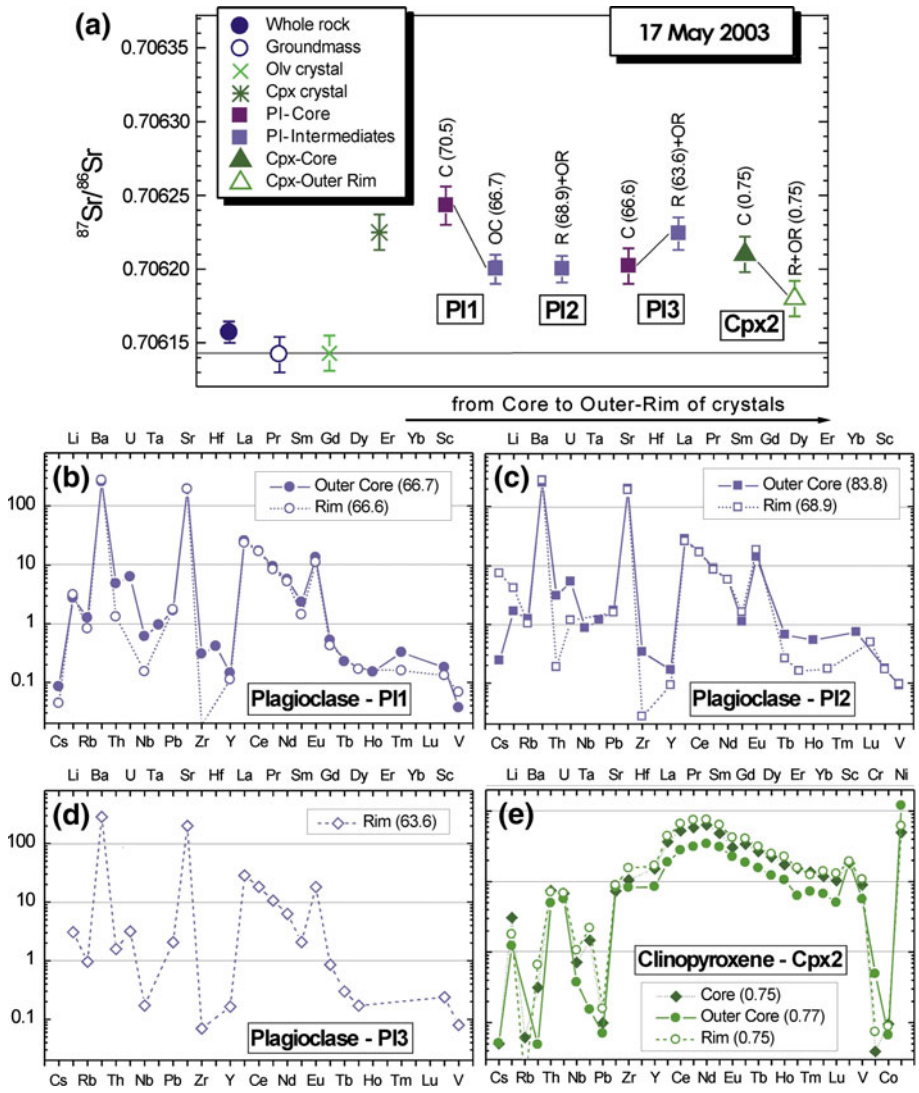

Fig. 7 **a** Micro-Sr-isotope ratios for core-rim traverses in clinopyroxene and plagioclase of the 17 May 2003 lava sample (STR170503). Sr-isotope data on separated clinopyroxene and olivine (*Olv*) crystals (*asterisk* and *cross*, respectively), on whole rock (*full circle*) and drilled groundmass (*open circle*) are also reported. Symbols and labels as in Fig. 4. **b, c, d, e** Chondrite-normalised trace element patterns for plagioclase (**b**, **c**, **d**) and clinopyroxene (**e**). See caption of Fig. 4 for details

mineral compositions of the Stromboli shoshonitic series (Fig. 9). Thus, the latter characteristic, together with the high Sr-isotope value (the pre-Neostromboli shoshonitic activity has Sr-isotope ratios lower than 0.70620, Fig. 1), constrain the provenance of the high Sr-isotope antecrysts from the Recent Period. The shoshonitic basalts of 'Pizzo-Sopra-la-Fossa tuff cone', in particular, have both the highest Sr-isotope ratios (up to 0.70669: Petrone et al. 2004; Di Salvo 2010) and the oldest age (~2.5 ka: Rosi et al. 2000; Speranza et al. 2008; Di Salvo 2010) of the whole Recent Period. This limits the crystallisation age of the antecrysts with the highest Sr-isotope ratios at a period not older than about 2.5 ka. On the other hand, the presence of antecrysts as old as 2.5 ka implies that the feeding system of Stromboli volcano and also its crystallisation conditions have been maintained during the last two millennia.

Furthermore, it is important to note that most of the $^{87}Sr/^{86}Sr$ values (~80%) measured in the high Sr-isotope antecrysts (defined as crystals with $^{87}Sr/^{86}Sr > 0.70618$) of the 2002–2003 products are lower than 0.70628. This value represents the most radiogenic Sr-isotope ratio registered in whole rocks and groundmasses during the twentieth century and possibly during the last 600 years (Francalanci et al. 1999, 2004 and unpublished; Speranza et al. 2008). This means that most of the antecrysts are likely crystallised in the last few hundred years and have been recycled by the dynamics of the present-day Strombolian activity.

Significance of the low Sr-isotope crystal zones

In a previous study, Francalanci et al. (2005) found low Sr-isotope crystal zones around the high Sr-radiogenic cores and in some cores of crystals from the 1984 and 1996 scoria. The similarity between the chemical (high An% for plagioclase or Mg# for clinopyroxene) and Sr-isotopic (low $^{87}Sr/^{86}Sr$) compositions of these crystal zones with crystals found within pumice samples of the same eruptions

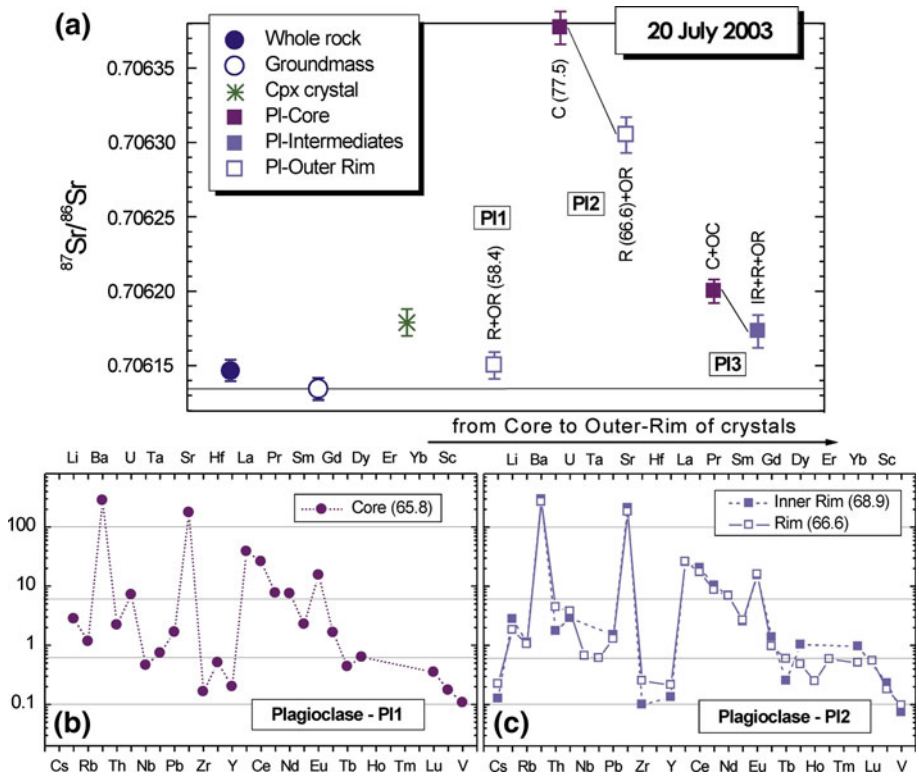

Fig. 8 **a** Micro-Sr-isotope ratios for core-rim traverses in plagioclase of the 20 July 2003 lava sample (STR200703). Sr-isotope data on a separated clinopyroxene (*Cpx*) crystal (*asterisk*), on whole-rock (*full circle*) and separated groundmass (*open circle*) are also reported. Symbols and labels as in Fig. 4. **b**, **c** Chondrite-normalised trace element patterns for plagioclase. See caption of Fig. 4 for details

suggested that low Sr-isotope zones crystallised from LP-magmas. In their interpretation, the replenishing LP-magma passed through the crystal mush reservoir, 'collected' the crystals carrying them into the HP-reservoir and contemporaneously crystallising low Sr-isotope crystal zones around the high Sr-radiogenic cores.

Amongst all the crystals measured in this study, only one crystal zone with lower $^{87}Sr/^{86}Sr$ (0.70597) than the relative groundmass (0.70615) (i.e. a low Sr-isotope crystal zone) was found within the internal part of the clinopyroxene-Cpx1 from 5 April 2003 scoria (Table 1a; Figs. 6a, 10). This crystal contains a large diopsidic outer core (Mg# 0.89) with a low incompatible element contents (Fig. 6e), suggesting it also crystallised from an LP-magma. As the lowest known $^{87}Sr/^{86}Sr$ value of LP-magmas is 0.70605 in 1996 products (Francalanci et al. 2005, 2008), the even lower $^{87}Sr/^{86}Sr$ value of Cpx-1 outer core can testify that the isotope composition of LP-magmas were even lower than 0.70605 at some stage in the recent history of the volcano.

On the contrary, we did not find any low Sr-isotope zone crystallised around the high Sr-radiogenic cores. This is possibly due to a sampling bias since these zones are quite thin and difficult to isolate by drilling. An example of this could be the Cpx2 of Figs. 7a,e, where an outer core with high-MgO and lower-REE contents is present between the drilled core and outer rim; unfortunately, this very light and thin zone could not be drilled, but it is likely to represent a potential low $^{87}Sr/^{86}Sr$ (see also the sketch of this crystal in Fig. 10). Another possibility is that the low Sr-isotope crystal zones are sampled together with the neighbouring zones, as also observed in the 1985 lava sample of Francalanci et al. (2005). An example of this case in the present data has been explained above ('Sr-isotope and trace element results') for the Pl2 of Fig. 2. It can be argued that the thin and sieved rim with high An content (An_{80}), micromilled together with the adjacent zones, could be crystallised in the LP-magmas, thus having low $^{87}Sr/^{86}Sr$. It is also probable that most of the inner crystal zones displaying lower Sr-isotope ratios than the respective external zones (e.g. Pl3 of 28 December 2002, Pl4 of 6 March 2003, Pl1 of 5 April 2003 scoria; Figs. 4, 5, 6) include low Sr-isotope crystal zones, crystallised by LP-magmas at some early stage of the entire history of the mineral.

An alternative way of evaluating the possible presence of low Sr-isotope crystal zones within the antecrysts of the 2002–2003 activity is through simple mass balance. In several lava samples, for example that of 28 December 2002 (Fig. 4a), the whole-rock $^{87}Sr/^{86}Sr$ is almost identical to the $^{87}Sr/^{86}Sr$ of groundmasses. These same samples, however, bear a consistent amount of antecrysts with high Sr-radiogenic zones (Fig. 4). Therefore, a certain amount of low Sr-isotope crystal zones are needed in order to balance the average higher Sr-isotope ratio of the antecrysts: otherwise, the whole-rock measurements would yield higher $^{87}Sr/^{86}Sr$ than the groundmass.

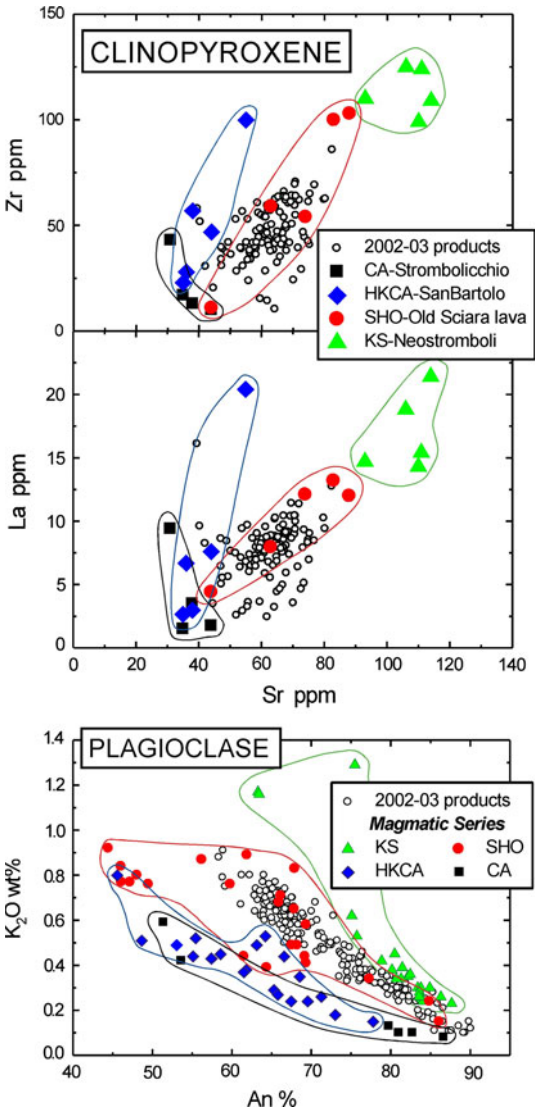

Fig. 9 Comparison of clinopyroxene and plagioclase compositions between the 2002–2003 products (data from the present paper and unpublished) and the older products of Stromboli volcano (*CA* calc-alkaline, *HKCA* high-K calc-alkaline, *SHO* shoshonitic, *KS* potassic series). Diagrams of Sr versus La and Zr contents for clinopyroxene and Anorthite content (An%) versus K_2O (wt%) for plagioclase. Clinopyroxene and plagioclase of the 2002–2003 products fall within the field of previous shoshonitic products. Older plagioclase data are from Francalanci (1993); clinopyroxene data are authors' unpublished data

We calculated the amount of Sr in the mineral assemblage (=1,000 ppm) from the difference between Sr content in the groundmass (500 ppm) and whole-rock (750 ppm), assuming a total crystal content of 50% in the whole rock, as derived from petrography. The required amount of low Sr-isotope crystal zones will thus depend on the $^{87}Sr/^{86}Sr$ values assumed for the two end-members. For the high Sr-isotope end-member, it is reasonable to use the average $^{87}Sr/^{86}Sr$ value calculated amongst all the high Sr-isotope antecrysts of 2002–2003 products (i.e. the average of 37 data higher than 0.70618 is 0.70624, which is nearly similar to the averages calculated in the single samples). For the low Sr-isotope end-member, the lowest value measured (0.70597) or the value of LP-magma erupted by the 5 April 2003 paroxysm (~0.70610) can be considered. Accordingly, we estimate that 30 or 50% of Sr, respectively, must derive from low Sr-isotope zones. Assuming a similar amount of low Sr-isotope zone in plagioclase and clinopyroxene, the above-mentioned estimates can refer to the relative volume of low Sr-isotope crystal zones. These estimates might seem in contrast with the scarcity of low Sr-isotope zones found and with their small size. However, it must be considered that low Sr-isotope zones are generally concentrated at the rim of the crystals; therefore, despite their limited area is difficult to sample by microdrilling, they actually represent a significant volume of the total crystals. In this light, the smaller value yielded by our calculation (~30%) might represent a reasonable estimate of the relative proportion of low to high Sr-radiogenic zones in the antecrysts. Thus, we suggest that LP-magmas with $^{87}Sr/^{86}Sr$ lower than that measured in the latest activity (5 April 2003) have entered the system at some stages.

The total amount of antecrysts can be broadly estimated at about 17% by petrography based on the observation that high Sr-isotope cores (antecrysts) are found in the most zoned crystals, which account for one-third of the total crystal content. This translated into total amounts of high and low Sr-isotope crystal zones of about 12 and 5% of the total rock, respectively.

Variations along the effusive event: interaction between LP- and HP-magmas

The whole-rock and mineral chemistry data on the 2002–2003 products show that the shallow magmatic system is still maintained in the steady-state conditions characteristic of the last decades. The general uniform bulk composition of the erupted lava indicates the presence of a considerable volume of homogeneous HP-magma residing in the shallow plumbing system of the volcano (an estimate of about 0.0088 km^3 has been calculated assuming ~30vol% lava vesicularity: Landi et al. 2006, 2008; Marsella et al. 2008).

The small but systematic decrease of the most incompatible trace element contents and Sr-isotope ratios in bulk rocks erupted after the 5 April paroxysm have been interpreted as generated by limited mixing (about 20%) between the fresh, volatile-rich LP-magma, erupted as pumice during the paroxysm, and the volatile-poor HP-magma feeding the lava flow (Landi et al. 2006, 2008). The micro-analytical data reported here allow

investigating this issue in detail. Indeed, a decreasing proportion of high Sr-isotope antecrysts would produce a consequent decrease in $^{87}Sr/^{86}Sr$ of whole rocks from the onset to the end lavas. However, the same trend is also observed in the groundmass analyses (Fig. 3). Since groundmass is obviously not affected by the amount or composition of the antecrysts, our data provide a clear evidence of the mixing of HP-magmas with increasing amount of low Sr-isotope LP-magmas similar to those erupted by the 5 April paroxysm. The amount of LP-magma mixed with HP-magma required for decreasing the $^{87}Sr/^{86}Sr$ values of the groundmass from the beginning (0.706161 ± 6) to the end (0.706134 ± 6) of the lava effusion is calculated at about 30%. This estimate must be halved considering that the groundmass accounts for roughly 50% of the whole rock.

It must be pointed out that whilst there is no difference between groundmass and whole-rock isotope composition in the onset lavas, this difference increases considerably after the 5 April and in particular in the end 20 July lava sample. This effect can only be explained by an increased amount of high Sr-isotope antecrysts. Assuming antecrysts with average Sr content of 1000 ppm and isotope ratio of 0.70624 (i.e. the average of data higher than 0.70618), this increase can be estimated at $\sim$8%. The higher amount of high Sr-isotope antecrysts towards the end lavas, associated with the decrease of $^{87}Sr/^{86}Sr$ in the groundmasses, could be brought in the shallow system by the increased arrival of LP-magmas passing through the crystal mush zone and carrying the previously formed crystals (Francalanci et al. 2005). This is further corroborated by the presence in the post-paroxysm lavas of high Sr-isotope antecrysts with outer rims in isotopic disequilibrium with the groundmass (Figs. 4, 5, 6, 7 and 8), suggesting a very short residence time for these antecrysts in the shallow system.

The above mixing calculations have been performed between the beginning and the end lavas. Nevertheless, the $^{87}Sr/^{86}Sr$ of the groundmasses begins to slightly but significantly decrease from February, to then decrease at a higher rate from May to July. Furthermore, the $^{87}Sr/^{86}Sr$ values of groundmasses in the scoria erupted by the 5 April paroxysm and in the following 14 April lavas are similar. This suggests that: (1) the arrival of LP-magmas at shallow levels and their mixing with HP-magmas seem to have also occurred before the 5 April paroxysm; (2) the rapid ascent of LP-magmas to the surface during the paroxysm does not immediately affect the composition of the shallow HP-magmas, even though the two magmas use the same conduit to the surface (Pistolesi et al. 2008 and reference therein). The evidence for point (1) is corroborated by the occurrence of a few LP glassy shards in ashes erupted on 8 March 2003 (Schiavi et al. 2010), together with changes in fluid geochemistry (Aiuppa and Federico 2004; Carapezza et al. 2004) and lowering of $^{87}Sr/^{86}Sr$ in scoria groundmasses (Landi et al. 2008) during October–November 2002. As for the consideration of point (2), it is also worth noting that the mineral bulk compositions and zoning patterns of post-paroxysm lavas do not change, maintaining the typical crystal outer-rim compositions in equilibrium with the HP-magmas (Francalanci et al. 2004; Landi et al. 2006, 2008); moreover, no variations in the crystal size distribution of lavas are found immediately after the paroxysm (Fornaciai et al. 2009).

Thus, different data indicate different processes: Sr-isotope ratios of groundmasses indicate that HP-magmas mixed with an increasing amount of LP-magmas from the beginning to the end of the effusive event, up to a maximum of 30% of LP-magmas in the 20 July lavas, although the mixing seems to be not directly related to the 5 April paroxysm. Petrographic and mineralogical characteristics, however, do not show the occurrence of this mixing process.

The present study reinforces the need for this shallow reservoir where efficient mixing between LP- and HP-magma occurs (Francalanci et al. 1999, 2004, 2005), as evident from the $^{87}Sr/^{86}Sr$ of the groundmass. Further degassing-driven crystallisation in the conduit leads to re-equilibration of the mineral compositions and the petrographic textures to those typical of HP-magmas producing $\sim$0.0088 km^3 (Landi et al. 2006; Marsella et al. 2008) of petrographically homogeneous lava. Furthermore, the presence of crystal outer rims in Sr-isotopic equilibrium with the mixed groundmass in the pre- and syn-paroxysm products indicates that their crystallisation occurred only after mixing (Figs. 4, 5, 6, 7, 8). In this frame, we can also attempt to constrain the timescale of this process. Assuming the maximum growth rate calculated for plagioclase crystals of Stromboli present-day activity (10^{-9}–10^{-8} cm/s; Armienti et al. 2008; Fornaciai et al. 2009), a 0.1-mm-large outer rim would form in a time ranging from several days to some months. This indicates that a considerable amount of LP-magma arrived in the shallow reservoir before the onset of the lava flows, as previously suggested.

Schiavi et al. (2010) report compositions of LP-magmas erupted as glassy shards in ash fallouts on 8 March 2003 and 10 April 2003. The latter are very similar to typical LP-magmas, whilst the former show higher contents of incompatible trace elements (intermediate between typical LP- and HP-matrix glass), Sr and Ni, Cr, V. The authors explain this anomalous LP-magma composition by fractional crystallisation of clinopyroxene and olivine associated with minor assimilation of dunite and wehrlite assemblages. This process is ascribed to a slow ascent rate to the surface favoured by LP-magma volumes that are smaller than during paroxysms. Our data suggest a possible alternative explanation. The pre-paroxysm LP-ash shards

could represent the ascent to the surface of an LP-magma already present in the shallow reservoir and thus partially mixed with HP-magma (leading to the increase in incompatible trace element contents). The increase in Cr, Ni, V and Sr contents can be due to resorption of previously crystallised minerals by the hotter LP-magmas. In the authors' hypothesis, small volume of LP-magmas would have continued to rise up from their deep reservoir during the effusive event, directly arriving at the surface (hence, no shallow reservoir is considered). In our alternative hypothesis, the pre-paroxysm LP-magmas would represent an early arrival of LP-magma in the shallow reservoir. The ascent of batches of this magma to the surface was allowed only after the decrease in the magmastatic pressure during the lava outpouring, hence leaving the time necessary for the incipient mixing shown in the anomalous composition of the erupted LP-glassy shards.

A new bigger input of typical LP-magma from the deep reservoir triggered the 5 April paroxysm by its direct arrival to the surface, passing through the conduit without mixing with the HP-magma due to the different rheology of the two magmas. A portion of the new LP-magma was left in the shallow reservoir and started to mix with the interstitial liquid of the HP-magma, leading to the further decrease in Sr-isotopes in the groundmasses of lavas erupted from May onwards. The new LP-magma input also brought more antecrysts ($\sim$8%) in the final lava system and the continuous lava outpouring to the surface inhibited the growth of outer rims in isotopic equilibrium. This apparently disagrees with the presence in post-paroxysm lavas of bulk olivine and clinopyroxene with Sr-isotope ratios similar to those of the host groundmass. However, the growth rate of olivine and clinopyroxene is respectively twice and four times higher than the plagioclase growth rate (Armienti et al. 2007) and the higher undercooling during the lava outpouring should have favoured the nucleation of these minerals, rather than antecryst rim growth, within the conduit and thus after mixing. Therefore, we suggest that these femic phases crystallise completely within the conduit.

Dynamics of the crystal recycling

Our data show the presence of high Sr-isotope antecrysts that record the variation of isotope composition of the magmas feeding the volcanic activity from the beginning of the Recent Period (2.5 ka) to the present day. Hence, the reservoir that hosts the antecrysts must be directly connected to and continuously sampled by the magmas of present-day activity. In a previous study, we suggested the presence of a cumulate crystal mush zone sited generically below the HP-magma reservoir, but still within the stability field of plagioclase (Francalanci et al. 2005). The new data presented here suggest that the connection between these two reservoirs (HP-magma and crystal mush) is more direct than previously thought (e.g. the crystal mush is part of the HP reservoir).

We could now suggest that the 'Pizzo-Sopra-la-Fossa' magma reservoir (shoshonitic basalts) represents the initial magma body of the HP-system. Its continuous crystallisation and refilling by lower Sr-radiogenic LP-magmas is responsible for both i) the general trend of decreasing $^{87}Sr/^{86}Sr$ with time and ii) the significant occurrence of high radiogenic-Sr antecrysts preserving the memory of the entire magma history in their different zones. This means that the plagioclase cores with the highest $^{87}Sr/^{86}Sr$ values (e.g. akin to 'Pizzo-Sopra-la-Fossa' magmas: 0.70665) have resided within the HP-magma system for about 2.5 ka. In such a period of time, Sr-isotopes would not equilibrate in over the lengthscales measured and at typical Stromboli temperatures (Davidson et al. 2007 and reference therein); therefore, each zone of the crystal would reflect equilibration with the melt entering the system at a certain time. Previous estimates of the residence times in the Stromboli magmatic systems, however, indicate much smaller timescales (<30 years: Gauthier and Condomines 1999; Francalanci et al. 1999). Hence, the old antecrysts must be periodically transferred into the HP-magma system by the refilling LP-magmas which pass through a cumulate crystal mush formed since the 'Pizzo-Sopra-la-Fossa' activity (Fig. 10). Accordingly, an increase in the antecryst amount is expected to be directly linked with major eruptions, reflecting the arrival of significant batches of fresh LP-magmas, as observed after the 5 April paroxysm.

Thus, we can now propose that the cumulate zone forms the lower part of the HP-magma shallow reservoir, being partially re-mobilised by the gas/volatile-rich LP-magmas, which periodically refill the HP-magma reservoir (Fig. 10).

Before mixing with HP-magmas, the external zones of the high Sr-isotope antecrysts can be resorbed by the host LP-magma crystallising new low Sr-isotope crystal zones in response to degassing at low pressure (Francalanci et al. 2005).

Furthermore, our calculations indicate that about 80% of antecrysts have isotope composition belonging to the last few hundred years, implying that they are recycled by the dynamic processes of the Strombolian activity. This mechanism has to be particularly efficient in recycling crystals considering the significant amount of these relatively recent antecrysts occurring in HP-magmas. It is nowadays believed that the periodic mild Strombolian explosions leave in the conduit a degassed dense HP-magma descending downwards possibly along the conduit walls (Chouet et al. 2003; Colò et al. 2010; Lautze and

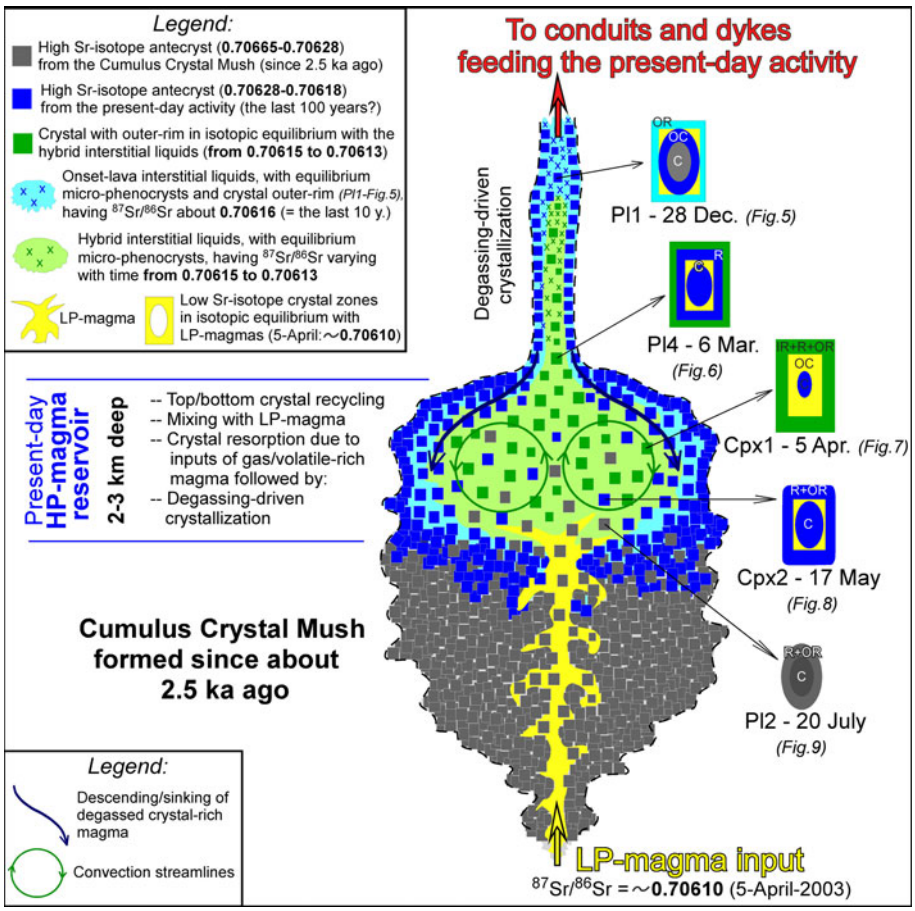

Fig. 10 Cartoon of the intermediate plumbing system (HP-magma reservoir and crystal mush zone) feeding the present-day activity of Stromboli during the 2002–2003 eruptive crisis. Based on the data reported in this paper, the picture represents an interpretative model of the shallow HP-magma reservoir and its relationship with a cumulate crystal mush zone sited below. Some significant crystal zoning, effectively found in the specified minerals, is schematically drawn as examples (*letters indicate* the drilled crystal-zones, *C* core, *OC* outer core, *IR* inner rim, *R* rim, *OR* outer rim). It is considered that a significant amount of LP-magmas arrived (before and possibly after the onset of the lava flow and during the 5 April paroxysm) and mixed in the shallow HP-magma reservoir, passing through a cumulate crystal mush zone, formed since the "Pizzo-Sopra-la-Fossa" activity (about 2.5 ka ago), and carrying high Sr-isotope antecrysts (grey squares) in the reservoir. High Sr-isotope antecrysts (blue squares) also form by the dynamic processes of the Strombolian activity, when descending degassed HP-magma sinks in the lower magmas and are recycled by convective movements. $^{87}Sr/^{86}Sr$ values of the different crystals, crystal zones, antecrysts and interstitial liquids are also written in figure. Other explanations are reported in the figure and in the text. The crystal size, the conduit width and length are not in *scale*. The relative aspect ratios of the HP-magma reservoir and crystal mush are hypothetical

Houghton 2007; Burton et al. 2007; Fornaciai et al. 2009; Metrich et al. 2010). This process leads minerals (with possibly degassed silicate melt) to be also recycled from the upper part of the plumbing system into the HP-magma reservoir. When minerals sink in a hotter, gas/volatile-richer melt (blue down arrows of Fig. 10), they suffer resorption at various extents depending on the conditions of the host melt (i.e. degree of mixing with LP-magmas, crystallisation and degassing) and possibly on their location in the reservoir. Obviously, low Sr-isotope crystal zone (i.e. in equilibrium with the LP-magma end-member) can only grow on crystals settled in the lower part of the magma body and re-mobilised again by LP-magma inputs (e.g., Cpx2 of Figs. 7, 10).

This intricate dynamics of crystal recycling, in which minerals (and possibly melts) re-enter in the convective portion of the HP-magma chamber from both lower and upper parts, leads to the complex and multiple zoning of many minerals of the products from the present-day activity (Fig. 10).

Magma volumes

Two of the evidences arisen in this study might be used for attempting some consideration on the magma volumes involved in the Stromboli system.

We previously pointed out the presence in 13 May and 17 May 2003 lavas of mafic phases crystallised in isotopic

equilibrium with an HP-liquid already affected by mixing with LP-magma (end of 'Variations along the effusive event: interaction between LP- and HP-magmas'). These mafic phases were interpreted as completely formed after the new input of fresh LP-magma in the shallow reservoir (5 April 2003 paroxysm), during the ascent in the conduit to the surface, hence in a timeframe of 30–40 days. This is consistent with the growth rate of 3×10^{-8} cm/s (the maximum growth rate according to Armienti et al. 2007) for a mafic phase of that size (about 1 mm). Since these crystals should have crystallised only in the conduit, their age (30–40 days) can be used for calculating the volume of the conduit if the eruption rates are known. Considering an average mass eruption rate of 0.7 m^3/s (i.e. the total lava volume divided for the entire period of lava effusion; Marsella et al. 2008), we can calculate a conduit volume of 0.002 km^3. This represents about 25% of the total lava volume erupted (0.0088 km^3; Landi et al. 2006; Marsella et al. 2008). Assuming the simplest geometry (i.e. cylinder) the conduit would have a length of about 2.5 km (i.e. above the 2–3 km deep HP-reservoir) and a diameter of 33 m. The estimates for length and width of the conduit are obviously increased and reduced, respectively, if more complex geometries (e.g., Chouet et al. 2008) are considered.

Another key characteristic of Stromboli 2002–2003 activity is the decrease of $^{87}Sr/^{86}Sr$ measured in the groundmass of HP-magmas from the onset to the end lavas. We modelled this variation as due to mixing with up to 30% of the low Sr-isotope LP-magma refilling the shallow HP-reservoir. This is a melt (LP) to melt (HP) proportion that can be converted in vol% of the total HP-reservoir (liquid to total volume) if the amount of crystallinity of the latter is known. The average crystallinity of Stromboli rocks is about 50%, but a considerable part of it occurs above the HP-reservoir in the conduit; it can be estimated that the crystallinity within the HP-reservoir is about 30% (hence the HP-melt constitutes 70% of the total reservoir). Therefore, when referred to the total volume of the shallow reservoir, the previously estimated amount of mixed LP-magmas (30%) must become ~20%. Thus, the actual volume of the LP-magma input can be deducted from the volume of the HP reservoir. Francalanci et al. (1999) provide two possible volumes (i.e. 0.04 or 0.3 km^3), based on two different evaluations of magma input flux at Stromboli (Giberti et al. 1992; Allard et al. 1994; Harris and Stevenson 1997). These values can be converted in two end-member volumes for the LP-magmas remained within the HP-reservoir, of 0.0084 km^3 or 0.063% km^3, respectively. Although there is no real possibility to choose rigorously between the two, we favour the smaller estimate, mainly based on the short time the bulk system takes to re-homogenise the composition (Francalanci, unpublished data). The smaller estimate (0.0084 km^3) turns out to be amazingly similar to the total volume of the erupted lavas (i.e. 0.0088 km^3; Landi et al. 2006; Marsella et al. 2008). This would be consistent with the HP-reservoir having a broadly constant volume, hence the lava flows representing the excess of magma overflowing the HP-reservoir after the arrival of significant amount of new LP one. The bigger estimate (0.063% km^3) would indicate instead a volume of the LP-magma input ~8 times greater that of the erupted lavas, which seems physically implausible. This is important because events of lava effusion not related to paroxysms can also be interpreted as related to the entrance of a comparable volume of fresh LP-magma from the deep reservoir, which, however, do not reach the surface. In fact, we can also attempt to assess the proportion of LP-magma erupted during the paroxysm with respect to that entering the shallow reservoir. Recent studies (Rosi et al. 2006; Pistolesi et al. 2008) provide estimates of the total volume of juvenile material erupted during the 5 April paroxysm. Combining their data, we calculated a maximum of 4.3×10^4 m^3 of DRE magma erupted, of which no more than 50% (probably less) can be of the LP-type. This converts into 2.2×10^{-5} km^3 of erupted LP-magma, which is less than 0.3% of the magma volume refilling the shallow reservoir (0.0084 km^3). Although the absolute numbers reported here are only indicative, due to the several sources of uncertainty affecting the volume calculations, the 0.3% figure was calculated using maxima and minima estimates for erupted (Rosi et al. 2006; Pistolesi et al. 2008) and input (Francalanci et al. 1999) volumes, respectively, hence it likely represents an overestimate. Therefore, our data strongly indicate that only a minor proportion of LP-magma input reaches directly the surface without residing in the shallow reservoir.

Conclusions

Several new contributions to the understanding of 2002–2003 eruptive crisis and to the present-day system of Stromboli arise from the numerous chemical and Sr-isotope micro-analytical data presented in this study. These new findings also provided insights into the configuration of the plumbing system of Stromboli. A sketch model of the revised plumbing system is shown in Fig. 10 and a summary of the major outcomes of the study is listed hereafter.

1. The presence of recycled minerals inherited from the previous activity (antecrysts) seems to be a constant characteristic of the present-day plumbing system (Figs. 4, 5, 6, 7, 8) which, together with the interaction between HP- and LP-magmas, allows the typical steady-state conditions of this volcanic system to be maintained.

2. The $^{87}Sr/^{86}Sr$ values of the high Sr-isotope antecrysts (0.70665–0.70618), along with their trace element composition, constrain their age to a period not older than about 2.5 ka, (Recent Period of activity) that starts with the emplacement of 'Pizzo-Sopra-la-Fossa' tuff cone and ends with the present-day activity (Figs. 4, 5, 6, 7, 8, 9).
3. Antecrysts (and possibly melts) re-enter in the HP-magma reservoir (sited about 2–3 km depth) from both its lower and upper parts. From the bottom, they are re-mobilised by ascending LP-magmas from a cumulate crystal mush reservoir possibly directly interconnected with the HP-magma reservoir. From the top, the degassed and dense HP-magma left in the conduit by the periodic mild Strombolian explosions, sinks into the hotter and gas/volatile-richer melts residing in the reservoir (Fig. 10).
4. The presence of low Sr-isotope crystal zones, grown in equilibrium with LP-magmas, is inferred in a proportion ~30:70 (wt%) between low:high Sr-isotope crystal zones. The one low Sr-isotope crystal zone drilled in the internal part of a clinopyroxene (Table 1; Figs. 6a, 10) testifies that the Sr-isotope ratios of previous LP-magmas could have been significantly low (0.70597), as confirmed by mass balance consideration. Based on petrographic observations, we roughly evaluate amounts of 12% of high Sr-isotope antecrysts and 5% of low Sr-isotope crystal zones on the whole-rock of the onset lava.
5. The abundance of high Sr-isotope antecrysts, however, increases towards the end lavas (~8%), likely in relationship with a new arrival of LP-magmas during the 5 April paroxysm.
6. The presence of mafic phases with isotope composition in equilibrium with an LP–HP mixed liquid testifies a fast (30–40 days) degassing-driven growth within the conduit. This also allows calculating an approximate conduit volume of 0.002 km^3 (~25% of the erupted lava volume).
7. The decrease in the groundmass isotope values from the beginning to the end of the effusive event testifies mixing of the HP-melt residing in the shallow reservoir with up to 30% of the LP-melt refilling the system. This along with the occurrence of plagioclase outer rims in equilibrium with already-mixed melts suggests that LP-magma was arriving in the shallow level reservoir even before the onset of the lava flow.
8. This estimate can be used to calculate the possible volumes of LP-magma input during the 2002–2003 crisis. This turns out to be very similar to the total volume of the erupted lavas, indicating a steady-state system at constant volume where the lava flows represent an overflow in response to the arrival of fresh LP-magma in the HP-magma reservoir.
9. The amount of LP-magma erupted during the 5 April paroxysm is trivial with respect to that entering the system during the 2002–2003 period (<0.3%).

Acknowledgments We sincerely thank the late Filippo Olmi for allowing access to EPMA facilities and for his skilful assistance during microprobe analyses. Mario Zaia (Zazà), Alpine guides of Stromboli and Soccorso Alpino of Guardia di Finanza from Nicolosi (Catania) are thanked for their field assistance during sampling. Chiara M. Petrone, Elena Boari, Simone Tommasini and Maurizio Ulivi are warmly thanked for helping and sharing time during isotope analyses. Sandro Conticelli is thanked for constant encouragement and final critical reading. The careful review of two anonymous referees greatly helped to improve the manuscript. Funding was provided by Italian Civil Defence through INGV-GNV and the European Commission of Energy, Environment and Sustainable Development, through ERUPT project (EVG1-CT2002-00058).

References

Aiuppa A, Federico C (2004) Anomalous magmatic degassing prior to the 5th April 2003 paroxysm on Stromboli. Geophys Res Lett 31:LI4607. doi:10.1029/2004GL020458

Aiuppa A, Federico C, Giudice G, Giuffrida G, Guida R, Gurrieri S, Liuzzo M, Moretti R, Papale P (2009) The 2007 eruption of Stromboli volcano: insights from real-time measurement of the volcanic gas plume CO_2/SO_2 ratio. J Volcanol Geotherm Res 182:221–230

Allard P (2010) A CO_2-rich gas trigger of explosive paroxysms at Stromboli basaltic volcano, Italy. J. Volcanol Geotherm Res 189:363–374

Allard P, Carbonnelle J, Métrich N, Loyer H, Zettwoog P (1994) Sulphur output and magma degassing budget of Stromboli volcano. Nature 368:326–330

Anders E, Grevesse N (1989) Abundances of the elements: meteoric and solar. Geochim Cosmochim Acta 53:197–214

Armienti P, Francalanci L, Landi P (2007) Textural effects of steady state behaviour of the Stromboli feeding system. J Volcanol Geotherm Res 160:86–98

Avanzinelli R, Boari E, Conticelli S, Francalanci L, Gualtieri L, Perini G, Petrone CM, Tommasini S, Ulivi M (2005) High precision Sr, Nd, and Pb isotopic analyses using new generation Thermal Ionisation Mass Spectrometer ThermoFinnigan Triton-Ti®. Period Miner 74(3):147–166

Barberi F, Rosi M, Sodi A (1993) Volcanic hazard assessment at Stromboli based on review of historical data. Acta Vulcanol 3:173–187

Bence AE, Albee AL (1968) Empirical correction factors for the electron microanalysis of silicates and oxides. J Geol 76:382–402

Bertagnini A, Métrich N, Landi P, Rosi M (2003) Stromboli an open window on the deep feeding system of a steady state volcano. J Geophys Res 108(B7):2336

Bertagnini A, Métrich N, Francalanci L, Landi P, Tommasini S, Conticelli S (2008) Volcanology and magma geochemistry of the present day activity: constraints on the feeding system. In: Calvari S, Inguaggiato S, Puglisi G, Ripepe M, Rosi M (eds) The Stromboli volcano—an integrated study of 2002–2003 eruption.

American Geophysical Union, Geophysical Monograph Series, vol 182, pp 19–37
Bonaccorso A, Cardaci C, Coltelli M, Del Carlo P, Falsaperla S, Panucci S, Pompilio M, Villari L (1996) Annual report of the world volcanic eruptions in 1993, Stromboli. Bull Volcanic Eruptions 33:7–13
Bonaccorso A, Calvari S, Garfi G, Lodato L, Patane D (2003) Dynamics of the December 2002 flank failure and tsunami at Stromboli volcano inferred by volcanological and geophysical observations. Geophys Res Lett 30:18. doi:10.1029/2003GL017702
Burgisser A, Bergantz GW (2011) A rapid mechanism to remobilize and homogenize highly crystalline magma bodies. Nature 471:212–215
Burton MR, Mader HM, Polacci M (2007) The role of gas percolation in quiescent degassing of persistently active basaltic volcanoes. Earth Planet Sci Lett 264:46–60
Carapezza ML, Inguaggiato S, Brusca L, Longo M (2004) Geochemical precursors of the activity of an open-conduit volcano: the Stromboli 2002–2003 eruptive events. Geophys Res Lett 31:L07620. doi:10.1029/2004GL019614
Charlier BLA, Ginibre C, Morgan D, Nowell GM, Pearson DG, Davidson JP, Ottley CJ (2006) Methods for the microsampling and high-precision analysis of strontium and rubidium isotopes at single crystal scale for petrological and geochronological applications. Chem Geol 232:114–133
Chouet B, Dawson P, Ohminato T, Martini M, Saccorotti G, Giudicepietro F, De Luca G, Milana G, Scarpa R (2003) Source mechanisms of explosions at Stromboli volcano, Italy, determined from moment tensor inversions of very-long-period data. J Geophys Res 108(B1):2109. doi:10.1029/2002ID001919
Chouet B, Dawson P, Martini M (2008) Upper conduit structure and explosion dynamics at Stromboli. In: Calvari S, Inguaggiato S, Puglisi G, Ripepe M, Rosi M (eds) The Stromboli volcano—an integrated study of 2002–2003 eruption. American Geophysical Union, Geophysical Monograph Series, vol 182, pp 81–92
Colò L, Ripepe M, Baker DR, Polacci M (2010) Magma vesiculation and infrasonic activity at Stromboli open conduit volcano. Earth Planet Sci Lett 292:274–280
Davidson JP, Tepley FJ III, Palacs Z, Meffan-Main S (2001) Magma recharge, contamination and residence times revealed by in situ laser ablation isotopic analysis of feldspar in volcanic rocks. Earth Planet Sci Letts 184:427–442
Davidson JP, Morgan DJ, Charlier BLA, Harlou R, Hora JM (2007) Microsampling and isotopic analysis of igneous rocks: implications for the study of magmatic system. Ann Rev Earth Planet Sci 35:273–311
De Fino M, La Volpe L, Falsaperla S, Frazzetta G, Neri G, Francalanci L, Rosi M, Sbrana A (1988) The Stromboli eruption of December 6, 1985–April 25, 1986: volcanological, petrological and seismological data. Rend Soc It Mineral Petrol 43:1021–1038
Di Carlo I, Pichavant M, Rotolo SG, Scaillet B (2006) Experimental crystallization of a high-K arc basalt: the golden pumice, Stromboli volcano (Italy). J Petrol 47:1317–1343
Di Salvo S (2010) "Pizzo Sopra la Fossa" volcanic activity at Stromboli: geochemical and isotopic data (in Italian). B.Sc. Thesis, Università degli Studi di Firenze
Fornaciai A, Landi P, Armienti P (2009) Dissolution/crystallization kinetics recorded in the 2002–2003 lavas of Stromboli (Italy). Bull Volcanol 71:631–641. doi:10.1007/s00445-008-0249-3
Francalanci L (1993) Mineral chemistry of Stromboli volcanics as indicator of magmatic processes. Acta Vulcanol 3:99–113
Francalanci L, Manetti P, Peccerillo A (1989) Volcanological and magmatological evolution of Stromboli volcano (Aeolian islands): the roles of fractional crystallisation, magma mixing, crustal contamination and source heterogeneity. Bull Volcanol 51:355–378
Francalanci L, Manetti P, Peccerillo A, Keller J (1993) Magmatological evolution of the Stromboli volcano (Aeolian Arc, Italy): inferences from major and trace element and Sr-isotopic composition of lavas and pyroclastic rocks. Acta Vulcanol 3:127–151
Francalanci L, Tommasini S, Conticelli S, Davies GR (1999) Sr isotope evidence for short magma residence time for the 20th century activity at Stromboli volcano, Italy. Earth Planet Sci Lett 167:61–69
Francalanci L, Tommasini S, Conticelli S (2004) The volcanic activity of Stromboli in the 1906–1998 period: mineralogical, geochemical and isotope data relevant to the understanding of Strombolian activity. J Volcanol Geotherm Res 131:179–211
Francalanci L, Davies GR, Lustenmhower W, Tommasini S, Mason PRD, Conticelli S (2005) Old crystal re-cycle and multiple magma reservoirs in the plumbing system of the present day activity at Stromboli volcano, South Italy: Sr-isotope in situ microanalyses. J Petrol 46:1997–2021. doi:10.1093/petrology/egi045
Francalanci L, Bertagnini A, Métrich N, Renzulli A, Vannucci R, Landi P, Del Moro S, Menna M, Petrone CM, Nardini I (2008) Mineralogical, geochemical and isotopic characteristics of the ejecta from the 5 April 2003 paroxysm at Stromboli, Italy: inferences on the pre-eruptive magma dynamics. In: Calvari S, Inguaggiato S, Puglisi G, Ripepe M, Rosi M (eds) The Stromboli volcano—an integrated study of 2002–2003 eruption. American Geophysical Union, Geophysical Monograph Series, vol 182, pp 331–345
Gauthier PJ, Condomines M (1999) 210Pb/226Ra radioactive disequilibria in recent lavas and radon degassing: inferences on the magma chamber dynamics at Stromboli and Merapi volcanoes. Earth Planet Sci Lett 172:111–126
Giberti G, Jaupart C, Sartoris G (1992) Steady-state operation of Stromboli volcano, Italy: constraints on the feeding system. Bull Volcanol 54:535–541
Gillot PY, Keller J (1993) Radiochronological dating of Stromboli. Acta Vulcanol 3:69–77
Harris AJL, Stevenson DS (1997) Magma budgets and steady state activity of vulcano and Stromboli. Geophys Res Lett 24:1043–1046
Harris AJL, Ripepe M, Calvari S, Lodato L, Spampinato L (2008) The 5 April 2003 explosion of Stromboli: timing of eruption dynamics using thermal data. In: Calvari S, Inguaggiato S, Puglisi G, Ripepe M, Rosi M (eds) The Stromboli volcano—an integrated study of 2002–2003 eruption. American Geophysical Union, Geophysical Monograph Series, vol 182, pp 305–316
Hornig-Kjarsgaard I, Keller J, Koberski U, Stadlbauer E, Francalanci L, Lenhart R (1993) Geology, stratigraphy and volcanological evolution of the island of Stromboli, Aeolian arc, Italy. Acta Vulcanol 3:21–68
Keller J, Hornig-Kjarsgaard I, Koberski U, Stadlbauer E, Lenhart R (1993) Geological map of the island of Stromboli—scale 1:10,000. Acta Vulcanol 3: appendix
Kokelaar P, Romagnoli C (1995) Sector collapse, sedimentation and clast population evolution at an active island-arc volcano: Stromboli, Italy. Bull Volcanol 57:240–262
Landi P, Métrich N, Bertagnini A, Rosi M (2004) Dynamics of magma mixing and degassing recorded in plagioclase at Stromboli (Aeolian Arcipelago, Italy). Contrib Mineral Petrol 147:213–227
Landi P, Francalanci L, Pompilio M, Rosi M, Corsaro RA, Petrone CM, Cardini I, Miraglia L (2006) The December 2002–July 2003 effusive event at Stromboli volcano, Italy: insights into the shallow plumbing system by petrochemical studies. J Volcanol Geotherm Res 155:263–284

Landi P, Francalanci L, Corsaro RA, Petrone CM, Fornaciai A, Carroll M, Nardini I, Miraglia L (2008) Textural and compositional characteristics of the lavas erupted in the December 2002–July 2003 effusive events at Stromboli, Aeolian Island, Italy. In: Calvari S, Inguaggiato S, Puglisi G, Ripepe M, Rosi M (eds) The Stromboli volcano—an integrated study of 2002–2003 eruption. American Geophysical Union, Geophysical Monograph Series, vol 182, pp 213–228

Landi P, Corsaro RA, Francalanci L, Civetta L, Miraglia L, Pompilio M, Tesoro R (2009) Magma dynamics during the 2007 Stromboli eruption (Aeolian Islands. Italy): mineralogical, geochemical and isotopic data. J Volcanol Geotherm Res 182:255–268

Lautze NC, Houghton BF (2007) Linking variable explosion style and magma textures during 2002 at Stromboli volcano, Italy. Bull Volcanol 69:445–460. doi:10.1007/s00445-006-0086-1

Marsella M, Coltelli M, Proietti C, Branca S, Monticelli R (2008) 2002–2003 lava flow eruption of Stromboli: a contribution to understanding lava discharge mechanisms using periodic digital photogrammetry surveys. In: Calvari S, Inguaggiato S, Puglisi G, Ripepe M, Rosi M (eds)The Stromboli volcano—an integrated study of 2002–2003 eruption. American Geophysical Union, Geophysical Monograph Series, vol 182, pp 229–246

Métrich N, Bertagnini A, Landi P, Rosi M (2001) Crystallization driven by decompression and water loss at Stromboli volcano (Aeolian Islands, Italy). J Petrol 42:1471–1490

Métrich N, Bertagnini A, Landi P, Rosi M (2005) Triggering mechanism at the origin of paroxysms at Stromboli (Aeolian Archipelago, Italy): the 5 April 2003 eruption. Geophys Res Lett 32:L10305. doi:10.1029/2004GL022257

Métrich N, Bertagnini A, Di Muro A (2010) Conditions of magma storage, degassing and ascent at Stromboli: new insights into the volcano plumbing system with inferences on the eruptive dynamics. J Petrol 51:603–626

Morelli C, Giese P, Cassinis R, Colombi B, Guerra I, Luongo G, Scarascia S, Shutte KG (1975) Crustal structure of Southern Italy. A seismic refraction profile between Puglia–Calabria–Sicily. Boll Geofis Teor Appl 18:183–210

Pasquarè G, Francalanci L, Garduño VH, Tibaldi A (1993) Structure and geologic evolution of the Stromboli volcano, Aeolian islands, Italy. Acta Vulcanol 3:79–89

Perini G, Tepley FJ III, Davidson JP, Conticelli S (2003) The origin of K-feldspar megacrysts hosted in alkaline potassic rocks from central Italy: a track for low-pressure processes in mafic magmas. Lithos 66:223–240

Petrone CM, Francalanci L, Braschi E (2004) Pyroclastic deposits associated with sector collapses at Stromboli volcano: inferences from mineralogical, geochemical and isotopic data. 32° international geological congress, Firenze, Abstracts, Part 1, vol 68–20, p 334

Petrone CM, Olmi F, Braschi E, Francalanci L (2006) Mineral chemistry profile: a valuable approach to unravel magma mixing processes in the recent volcanic activity of Stromboli, Italy. Period Mineral 75:277–292

Pistolesi M, Rosi M, Pioli L, Renzulli A, Bertagnini A, Andronico D (2008) The paroxysmal explosion and its deposits. In: Calvari S, Inguaggiato S, Puglisi G, Ripepe M, Rosi M (eds) The Stromboli volcano—an integrated study of 2002–2003 eruption. American Geophysical Union, Geophysical Monograph Series, vol 182, pp 317–330

Puglisi G, Bonaccorso A, Mattia M, Aloisi M, Bonforte A, Campisi O, Cantarero M, Falzone G, Puglisi B, Rossi M (2005) New integrated geodetic monitoring system at Stromboli volcano (Italy). Engineer Geol 79:13–31

Ramos FC, Wolff JA, Tollstrup DL (2004) Measuring $^{87}Sr/^{86}Sr$ variations in minerals and groundmass from basalts using LA-MC-ICPMS. Chem Geol 211:135–158

Ripepe M, Harris AJL, Carniel R (2002) Thermal, seismic and infrasonic evidences of variable degassing rates at Stromboli volcano. J Volcanol Geotherm Res 118:285–297

Ripepe M, Marchetti E, Ulivieri G, Harris A, Dehn J, Burton M, Caltabiano T, Salerno G (2005) Effusive to explosive transition during the 2003 eruption of Stromboli volcano. Geology 33(5):341–344

Ripepe M, Delle Donne D, Harris AJL, Marchetti E, Ulivieri G (2008) Dynamics of Strombolian activity. In: Calvari S, Inguaggiato S, Puglisi G, Ripepe M, Rosi M (eds) The Stromboli volcano—an integrated study of 2002–2003 Eruption. American Geophysical Union, Geophysical Monograph Series, vol 182, pp 39–48. doi: 10.1029/182GM05

Rosi M, Bertagnini A, Landi P (2000) Onset of the persistent activity at Stromboli volcano (Italy). Bull Volcanol 62:294–300

Rosi M, Bertagnini A, Harris AJL, Pioli L, Pistolesi M, Ripepe M (2006) A case history of paroxysmal explosion at Stromboli: timing and dynamics of the April 5, 2003 event. Earth Planet Sci Lett 243:594–606

Schiavi F, Kobayashi K, Moriguti T, Nakamura E, Pompilio M, Tiepolo M, Vannucci R (2010) Degassing, crystallization and eruption dynamics at Stromboli: trace element and lithium isotopic evidence from 2003 ashes. Contrib Mineral Petrol 159:541–561

Spampinato L, Calvari S, Harris AJL, Dehn J (2008) Evolution of the lava flow field by daily thermal and visible airborne surveys. In: Calvari S, Inguaggiato S, Puglisi G, Ripepe M, Rosi M (eds) The Stromboli volcano—an integrated study of 2002–2003 eruption. American Geophysical Union, Geophysical Monograph Series, vol 182, pp 201–212

Speranza F, Pompilio M, D'Ajello Caracciolo F, Sagnotti L (2008) Holocene eruptive history of the Stromboli volcano: constraints from paleomagnetic dating. J Geophys Res 113. doi: 10.1029/2007JB005139

Tepley FJ III, Davidson JP (2003) Mineral-scale Sr-isotope constraints on magma evolution and chamber dynamics in the Rum layered intrusion, Scotland. Contrib Mineral Petrol 145:628–641

Tepley FJ III, Davidson JP, Tilling RI, Arth JG (2000) Magma mixing, recharge and eruption histories recorded in plagioclase phenocrysts from El Chichòn volcano, Mexico. J Petrol 41:1397–1411

Thirlwall MF (1991) Long-term reproducibility of multicollector Sr and Nd ratio analyses. Chem Geol 94:85–104

Tibaldi A (2001) Multiple sector collapses at Stromboli volcano: how they work. Bull Volcanol 63:112–125

Tommasi P, Baldi P, Chiocci FL, Coltelli M, Marsella M, Pompilio M, Romagnoli C (2005) The landslide sequence induced by the 2002 eruption at Stromboli volcano. In: Landslide—risk analysis and sustainable disaster management, chapter 32. Springer, pp 251–258

Vaggelli G, Olmi F, Conticelli S (1999) Evaluation of analytical errors during microprobe analyses of silicate minerals international reference samples. Acta Vulcanol 11:297–303

Vaggelli G, Francalanci L, Ruggieri G, Testi S (2003) Persistent polybaric rests of calc-alkaline magmas at Stromboli volcano, Italy: pressure data from fluid inclusions in restitic quartzite nodules. Bull Volcanol 65:385–404

van Achterbergh E, Ryan CG, Jackson SE, Griffin W (2001) Data reduction software for LA-ICP-MS. In: Sylvester P (ed) Laser ablation-ICPMS in the earth science. Mineral Associat Canada, vol 29, pp 239–243